Perturbativity constraints on U(1)$_{B-L}$ and left-right models and implications for heavy gauge boson searches

Garv Chauhan,[a] **P.S. Bhupal Dev,**[a] **Rabindra N. Mohapatra**[b] **and Yongchao Zhang**[a,c]

[a]*Department of Physics and McDonnell Center for the Space Sciences, Washington University,*
St. Louis, MO 63130, U.S.A.

[b]*Maryland Center for Fundamental Physics, Department of Physics, University of Maryland,*
College Park, MD 20742, U.S.A.

[c]*Center for High Energy Physics, Peking University,*
Beijing 100871, China

E-mail: garv.chauhan@wustl.edu, bdev@wustl.edu,
rmohapat@physics.umd.edu, yongchao.zhang@physics.wustl.edu

ABSTRACT: We derive perturbativity constraints on beyond standard model scenarios with extra gauge groups, such as SU(2) or U(1), whose generators contribute to the electric charge, and show that there are both upper and lower limits on the additional gauge couplings, from the requirement that the couplings remain perturbative up to the grand unification theory (GUT) scale. This leads to stringent constraints on the masses of the corresponding gauge bosons and their collider phenomenology. We specifically focus on the models based on SU(2)$_L$ × U(1)$_{I_{3R}}$ × U(1)$_{B-L}$ and the left-right symmetric models based on SU(2)$_L$ × SU(2)$_R$ × U(1)$_{B-L}$, and discuss the implications of the perturbativity constraints for new gauge boson searches at current and future colliders. In particular, we find that the stringent flavor constraints in the scalar sector of left-right model set a lower bound on the right-handed scale $v_R \gtrsim 10$ TeV, if all the gauge and quartic couplings are to remain perturbative up to the GUT scale. This precludes the prospects of finding the Z_R boson in the left-right model at the LHC, even in the high-luminosity phase, and leaves only a narrow window for the W_R boson. A much broader allowed parameter space, with the right-handed scale v_R up to $\simeq 87$ TeV, could be probed at the future 100 TeV collider.

KEYWORDS: Beyond Standard Model, Neutrino Physics

ArXiv ePrint: 1811.08789

Contents

1 Introduction

The standard model (SM) of particle physics is astonishingly successful as a theory of particles and forces in the Universe. However, to account for several observations, such as the tiny neutrino masses, nature of the dark matter and the origin of matter in the universe, the SM has to be extended to include new physics. Beyond the standard model (BSM) physics could of course be at any scale; however, from an experimental point of view, it is interesting if it is at the TeV scale so that it could be tested by current and planned experiments. Many TeV-scale BSM extensions proposed to remedy the above shortcomings of the SM introduce extended gauge groups, such as extra U(1) or SU(2)×U(1) groups at the TeV scale, which are usually derived from a higher symmetry group, such as SO(10) [1–5] at the grand unification theory (GUT) scale. Such extensions broadly fall into two classes:

  (i) The generators of the extra gauge groups contribute to the electric charge [6, 7]. Two widely discussed examples are (a) the models based on the gauge group SU(2)$_L$ × U(1)$_{I_{3R}}$ × U(1)$_{B-L}$ [8, 9] and (b) the left-right symmetric model (LRSM) based on the gauge group SU(2)$_L$ × SU(2)$_R$ × U(1)$_{B-L}$ [10–12], both of which are useful and motivated in order to understand neutrino masses via the seesaw mechanism [13–17].

  (ii) The extra gauge groups do not contribute to electric charge. Examples of this class are the dark photon [18–20], U(1)$_{B-L}$ [21, 22], and more generic U(1)$_X$ [23–26] models, which have been discussed extensively in connection with dark matter [27] and collider signatures [28].

In both these classes of models, demanding that gauge couplings remain perturbative i.e. $g_i < \sqrt{4\pi}$ up to the GUT or Planck scale imposes severe constraints on the allowed values of the extra gauge couplings, as well as on the masses of the additional gauge bosons. In case (i), where the additional group generators contribute to the electric charge, we find both upper and lower limits on the gauge couplings, whereas in case (ii), where the additional gauge couplings are not related to the electric charge, we only get upper limits and no lower limits. In this paper, we only focus on the case (i) models and derive the perturbativity bounds on the gauge couplings g_R and g_{BL}, corresponding to the $SU(2)_R$ (or $U(1)_{I_{3R}}$) and $U(1)_{B-L}$ gauge groups, respectively.

Our results have far-reaching implications for collider searches for extra gauge bosons. In particular, they have to be taken into consideration, while interpreting the current direct search constraints on the W_R [29, 30] and Z_R [31, 32] bosons from the Large Hadron Collider (LHC) data, or the prospects [33–37] at the High-Luminosity LHC (HL-LHC) and a future 100 TeV collider [38, 39]. In particular, if the measured gauge couplings fall outside the limits derived from perturbativity up to the GUT (or Planck) scale, that would imply that there is new physics at the TeV or intermediate scale which allows this to happen. That would have interesting implications for new BSM physics.

There is another important implication of our results for the LRSM. Due to the stringent flavor-changing neutral current (FCNC) constraints in the high-precision electroweak data such as $K_0 - \overline{K}_0$, $B_d - \overline{B}_d$ and $B_s - \overline{B}_s$ mixings [40], the parity partner of the SM doublet scalar is required to be very heavy, i.e. $\gtrsim 10$ TeV [41–44].[1] Then one of the quartic couplings (α_3) in the scalar potential [see eq. (4.5)] is of order one, if the right-handed (RH) scale v_R lies in the few-TeV range. As a result, the perturbativity of the quartic couplings up to the GUT scale imposes a lower bound on the v_R scale, i.e. $v_R \gtrsim 10$ TeV. The renormalization group (RG) running of α_3 and other quartic couplings involves the gauge couplings g_R and/or g_{BL}. Hence, the perturbativity constraints in the scalar sector of LRSM do not only narrow down significantly the allowed ranges for the gauge couplings g_R and g_{BL}, but also supersede the current W_R and Z_R mass limits from the LHC, and even rule out the possibility of finding them at the HL-LHC (see figure 7). Therefore, if a heavy W_R and/or Z_R boson was to be found at the later stages of LHC, then either it does not belong to the LRSM, or the minimal LRSM has to be further extended at the TeV-scale or a higher intermediate scale, such that all the gauge, scalar and Yukawa couplings are perturbative up to the GUT scale.

Though we focus on the minimal $U(1)_{B-L}$ and LRSM gauge groups in this paper, the basic arguments and main results could easily be generalized to other gauge groups at the TeV scale, such as the $SU(3)_L \times U(1)_X$ [45–48], $SU(3)_L \times SU(3)_R \times U(1)_X$ [49–53], and alternative left-right models with universal seesaw mechanism for the SM quarks and charged leptons [54–63] or with a stable right-handed neutrino (RHN) dark matter [64, 65]. However, our results do not apply to situations where the extra $U(1)$ groups emerge out of non-Abelian groups at an intermediate scale, since they will completely alter the ultraviolet

---

[1]Due to sizable hadronic uncertainties, the FCNC constraints on the heavy bidoublet scalars might go up to ~ 25 TeV.

(UV) behavior of the TeV scale U(1) gauge couplings. String theories provide many examples where extra U(1)'s persist till the string scale without necessarily being embedded in intermediate scale non-Abelian groups [28, 66]. However, if the extra TeV-scale gauge group in question is valid up to the GUT scale, where it gets embedded into a non-Abelian GUT group, SO(10) [1–5] or higher rank groups, our results will be applicable and give useful information on the particle spectrum at the TeV scale.

This paper is organized as follows: in section 2, we sketch the basic theoretical arguments behind the perturbativity constraints on the gauge couplings that contribute to the electric charge. The application to the $\mathrm{SU}(2)_L \times \mathrm{U}(1)_{I_{3R}} \times \mathrm{U}(1)_{B-L}$ gauge group is detailed in section 3, along with the implications for searches of the heavy Z_R boson and the v_R scale at the LHC and future 100 TeV colliders. The analogous study for the LRSM gauge group $\mathrm{SU}(2)_L \times \mathrm{SU}(2)_R \times \mathrm{U}(1)_{B-L}$ is performed in section 4, where we also include the phenomenological implications on the W_R, Z_R searches at colliders. We conclude in section 5. The state-of-the-art two-loop RG equations for the gauge, quartic and Yukawa couplings in the LRSM are collected in appendix A.

2 Theoretical constraints

Our basic strategy is as follows: in the SM, when the electroweak gauge group breaks down to the electromagnetic group, i.e. $\mathcal{G}_{\mathrm{SM}} \equiv \mathrm{SU}(2)_L \times \mathrm{U}(1)_Y \to \mathrm{U}(1)_{\mathrm{EM}}$, the electric charge is given by

$$Q = I_{3L} + \frac{Y}{2} \, , \tag{2.1}$$

and we have the relation among the gauge couplings at the electroweak scale:

$$\frac{1}{e^2} = \frac{1}{g_L^2} + \frac{1}{g_Y^2} \, , \tag{2.2}$$

where g_L, g_Y, e are the gauge couplings for the $\mathrm{SU}(2)_L$, $\mathrm{U}(1)_Y$ and $\mathrm{U}(1)_{\mathrm{EM}}$ gauge groups, respectively. Current experiments completely determine these coupling values at the electroweak scale [40]:

$$e = 0.313 \pm 0.000022 \, , \qquad g_L = 0.652 \pm 0.00026 \, , \qquad g_Y = 0.357 \pm 0.000060 \, . \tag{2.3}$$

When the SM is extended in the gauge sector, to the gauge group $\mathrm{SU}(2)_L \times \mathrm{U}(1)_X \times \mathrm{U}(1)_Z$, such that the extra $\mathrm{U}(1)_{X,Z}$'s both contribute to the electric charge, then the modified electric charge formula becomes

$$Q = I_{3L} + I_X + I_Z \, . \tag{2.4}$$

This is also true if we replace one of the $\mathrm{U}(1)_{X,Z}$'s with an SU(2). The corresponding relation involving the new gauge couplings become [67]:[2]

$$\frac{1}{g_Y^2} = \frac{1}{g_X^2} + \frac{1}{g_Z^2} \, , \tag{2.5}$$

---

[2]Note that we are not using here any GUT normalizations for the U(1) couplings in eq. (2.5). For normalized couplings, the relation has to be altered accordingly.

where g_X and g_Z are the gauge couplings for the $U(1)_X$ and $U(1)_Z$ gauge groups, respectively. This relation holds at the scale v_X, where $U(1)_X \times U(1)_Z$ breaks down to the SM $U(1)_Y$ and correlates the couplings $g_{X,Z}$ to g_Y. Since the value of g_Y is experimentally determined at any scale v_X (with the appropriate SM RG evolution), we must have $g_{X,Z}$ bounded from below in order to satisfy eq. (2.5). On the other hand, requiring that the gauge couplings $g_{X,Z}$ remain perturbative till the GUT or Planck scale implies that $g_{X,Z}$ must also be bounded from above at any given scale v_X. In other words, the couplings $g_{X,Z}$ can neither be arbitrarily large nor arbitrarily small at the TeV-scale, allowing only a limited range for their values. This in turn constrains the mass of the extra heavy gauge boson Z', which is given by $M_{Z'}^2 \sim (g_X^2 + g_Z^2)v_X^2$. Clearly this has implications for the production of Z' at colliders.

As an example, when the SM gauge group is extended to $SU(2)_L \times U(1)_{I_{3R}} \times U(1)_{B-L}$ as in section 3, or to $SU(2)_L \times SU(2)_R \times U(1)_{B-L}$ as in section 4, the gauge couplings $g_{X,Z}$ are respectively g_R and g_{BL}, and v_R is the scale at which the extended gauge groups break down to the SM electroweak gauge group $\mathcal{G}_{SM}$.

$$r_g \equiv \frac{g_R}{g_L} > \tan\theta_w \left(1 - \frac{4\pi}{g_{BL}^2} \frac{\alpha_{EM}}{\cos^2\theta_w}\right)^{-1/2}, \tag{2.6}$$

where $\theta_w \equiv g_Y/g_L$ is the weak mixing angle, and $\alpha_{EM} \equiv e^2/4\pi$ is the fine-structure constant. For a phenomenologically-preferred TeV-scale v_R, if g_{BL} is in the perturbative regime, we can set an *absolute* theoretical lower bound on $r_g > \tan\theta_w \simeq 0.55$ [68, 69]. One should note that the lower bound on g_R depends on the v_R scale. This is before requiring the perturbativity to persist up to the GUT or Planck scale. When perturbativity constraints are imposed, the lower limit on g_R becomes more stringent, as we show below (see figures 3, 4, 7 and 8).

3 $U(1)_{B-L}$ model

The first case we focus on is the $SU(2)_L \times U(1)_{I_{3R}} \times U(1)_{B-L}$ model [8, 9] which possesses two BSM $U(1)$ gauge groups, i.e. $U(1)_{I_{3R}} \times U(1)_{B-L}$, which break down to the SM $U(1)_Y$ at a scale v_R. Labeling the gauge couplings for the groups $U(1)_{I_{3R}}$ and $U(1)_{B-L}$ as g_R and g_{BL} respectively, we can set lower bounds on both g_R and g_{BL} at the v_R scale from the coupling relation (2.5), as well as upper bounds from the requirement that they remain perturbative up to the GUT scale, as argued in section 2.

The particle content of this model [70, 71] is presented in table 1. Freedom from anomalies requires three RHNs which help to generate the tiny neutrino masses via the type-I seesaw mechanism [14]. In the scalar sector, one singlet Δ_R is used to beak the $U(1)$ groups and generate the RHN masses, while the doublet H breaks the electroweak group, as in the SM. The one-loop renormalization group equations (RGEs) for the gauge couplings of the two $U(1)$'s are generated by the following β-functions:

$$16\pi^2 \beta(g_{I_{3R}}) = \frac{9}{2} g_{I_{3R}}^3, \tag{3.1}$$

$$16\pi^2 \beta(g_{BL}) = 3 g_{BL}^3. \tag{3.2}$$

	$SU(2)_L$	$U(1)_{I_{3R}}$	$U(1)_{B-L}$
Q	**2**	0	$\frac{1}{3}$
u_R	**1**	$+\frac{1}{2}$	$\frac{1}{3}$
d_R	**1**	$-\frac{1}{2}$	$\frac{1}{3}$
L	**2**	0	-1
N	**1**	$+\frac{1}{2}$	-1
e_R	**1**	$-\frac{1}{2}$	-1
H	**2**	$-\frac{1}{2}$	0
Δ_R	**1**	-1	2

Table 1. Particle content of the $SU(2)_L \times U(1)_{I_{3R}} \times U(1)_{B-L}$ model.

Note that we have not used GUT renormalized g_{BL}, since we are not considering coupling unification, but rather the implications for the heavy Z_R boson searches at colliders. This model could be viewed in some sense as an "effective" TeV-scale theory of LRSM with the $SU(2)_R$-breaking scale and the mass of the heavy W_R boson at the GUT scale [70, 71]. The $U(1)_{B-L}$ model discussed in this section could also be the TeV-scale effective theory of some GUT that contains $U(1)_{B-L}$ as a subgroup.

As an illustration, we set explicitly the RH scale $v_R = 5\,\text{TeV}$, and run the SM coupling g_Y from the electroweak scale M_Z up to the v_R scale, at which the couplings g_R and g_{BL} are related to g_Y as in eq. (2.5) and can be expressed as functions of the ratio $r_g \equiv g_R/g_L$. Then we evolve the two couplings g_R and g_Y from the v_R scale up to the GUT scale, based on the β-functions in eqs. (3.1) and (3.2). The correlations of $g_{R,BL}$ at the RH scale v_R and GUT scale $M_{\text{GUT}} = 10^{16}\,\text{GeV}$ are presented in figure 1, as functions of the ratio r_g at the v_R scale (as shown by the color coding). The horizontal shaded region is excluded by the perturbativity limit $g_{R,BL} < \sqrt{4\pi}$. The vertical dashed lines denote the upper limits on the gauge couplings, requiring them to stay below the perturbativity limit up to the GUT scale. On the other hand, the vertical dotted lines denote the lower limits on the gauge couplings, obtained from eq. (2.5), which implies there is only one degree of freedom in the $U(1)_{B-L}$ model, and the values of g_R and g_{BL} are correlated at the scale v_R, as shown by the red curve in figure 2. In other words, a lower bound on g_R corresponds to an upper bound on g_{BL}, and vice versa. Numerically, the gauge couplings are found to be constrained to lie within a narrow window

$$0.398 < g_R < 0.768 \ \text{ and } \ 0.416 < g_{BL} < 0.931 \,, \quad \text{with} \quad 0.631 < r_g < 1.218 \qquad (3.3)$$

at the v_R scale, as shown in figure 1.

The perturbativity constraints on the gauge couplings g_R and g_{BL} at the v_R scale have profound implications for the searches of the heavy Z_R boson, whose mass is given by

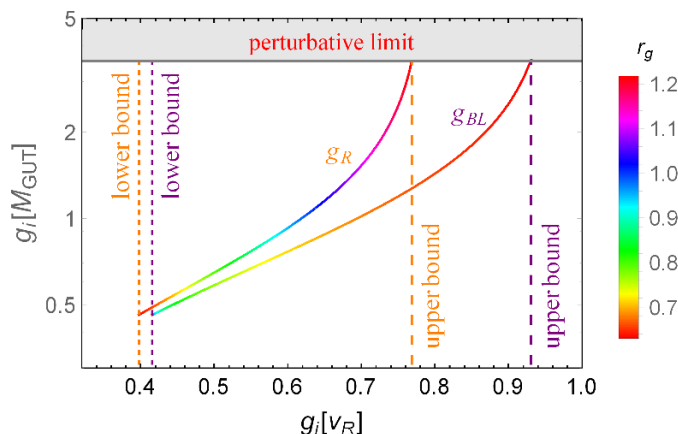$$M_{Z_R}^2 \simeq 2(g_R^2 + g_{BL}^2)\, v_R^2 \,. \qquad (3.4)$$

Figure 1. Correlation of $g_{R, BL}(v_R)$ and $g_{R, BL}(M_{\rm GUT})$ in the $U(1)_{B-L}$ model as functions of $r_g \equiv g_R/g_L$ at the v_R scale (shown by the color coding). The horizontal shaded region is excluded by the perturbativity limit $g_{R, BL} < \sqrt{4\pi}$. The vertical dotted and dashed lines respectively denote the lower and upper limits on the gauge couplings. Here we have chosen $v_R = 5\,{\rm TeV}$ and $M_{\rm GUT} = 10^{16}\,{\rm GeV}$.
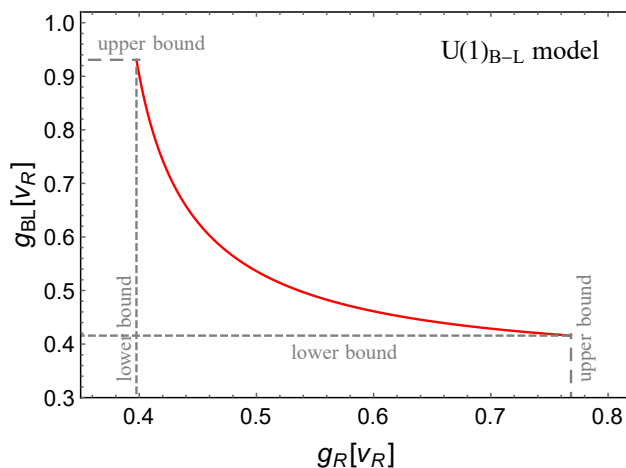

Figure 2. Correlation of g_R and g_{BL} at the scale $v_R = 5\,{\rm TeV}$ (red line) and the lower and upper bounds on the couplings g_R and g_{BL}, induced from the requirement of perturbativity up to the GUT scale in the $U(1)_{B-L}$ model.

The Z_R couplings to the chiral fermions $f_{L,R}$ are respectively [71]

$$g_{Z_R f_L f_L} = \frac{e}{\cos\theta_w} \left(I_{3,f} - Q_f\right) \frac{\sin\phi}{\cos\phi}, \tag{3.5}$$

$$g_{Z_R f_R f_R} = \frac{e}{\cos\theta_w} \left(I_{3,f} - Q_f \sin^2\phi\right) \frac{1}{\sin\phi\cos\phi} \tag{3.6}$$

with Q_f the electric charge of fermion f, $I_{3,f}$ the third-component of isospin of that particle, and $\tan\phi \equiv g_{BL}/g_R$ the RH gauge mixing angle.

For a TeV-scale v_R, the Z_R mass is stringently constrained by the dilepton data $pp \to Z_R \to \ell^+\ell^-$ (with $\ell = e, \mu$) at the LHC [72, 73]. For a sequential Z' boson, the current

collider	M_{Z_R} [TeV]	v_R [TeV]
LHC13	[3.6, 4.2]	[3.02, 3.57]
HL-LHC	[6.0, 6.6]	[4.60, 5.82]
FCC-hh	[27.9, 31.8]	[19.9, 26.8]

Table 2. The lower bounds on the Z_R boson mass M_{Z_R} and the v_R scale in the U(1)$_{B-L}$ model from the current LHC13 data [31, 32] and the prospects at the HL-LHC 14 TeV with an integrated luminosity of $3000\,\text{fb}^{-1}$ [74, 75] and future 100 TeV collider FCC-hh with a luminosity of $30\,\text{ab}^{-1}$ [34, 75]. The range in each case corresponds to the allowed range of r_g from perturbativity constraints, as given in eq. (3.3).

mass limit is 4.05 TeV at the 95% confidence level (CL) [31, 32]. The dilepton prospects of a sequential Z' boson have also been estimated at the HL-LHC [74, 75] and future 100 TeV colliders [34, 75], which are respectively 6.4 TeV and 30.7 TeV, for an integrated luminosity of $3000\,\text{fb}^{-1}$. Given a luminosity of 10 times larger at the 100 TeV collider, the dilepton prospects could be significantly enhanced, up to 43.7 TeV. The production cross section $\sigma(pp \to Z_R \to \ell^+\ell^-)$ in the U(1)$_{B-L}$ model can be obtained by rescaling that of a sequential heavy Z' boson, as function of $r_g = g_R/g_L$. The rescaled current mass limit and the expected limits at the HL-LHC and the future 100 TeV collider FCC-hh are presented in figure 3, as a function of r_g. The Z_R mass contours for $v_R = 5$, 10, 20 and 50 TeV are also shown in figure 3 in the colors of pink, green, blue and purple, respectively. The vertical shaded regions are excluded by the perturbativity constraints given in eq. (3.3).[3] Figure 3 implies that the LHC13 lower limits, as well as the future HL-LHC and FCC-hh limits, on Z_R boson mass are in a narrow range, depending on the allowed values of r_g, as shown in table 2. Thus, the perturbativity constraints restrict the accessible range of M_{Z_R} up to 6.6 TeV at the HL-LHC and 31.8 TeV at the FCC-hh. For the purpose of concreteness, we have assumed the decay $Z_R \to N_i N_i$ is open, such that the BR($Z_R \to \ell^+\ell^-$) is slightly smaller than the case without the decaying of Z_R into RHNs and the dilepton limits in figure 3 are comparatively more conservative [64].

The dilepton constraints on the Z_R mass can be traded for the constraints on v_R scale using eq. (3.4). This is shown in figure 4 and table 2. The pink, green, blue and purple contours here show the variation of v_R with respect to r_g, with fixed Z_R mass of $M_{Z_R} = 5$, 10, 20, 50 TeV, respectively. The perturbativity constraints given in eq. (3.3) restrict the accessible range of v_R up to 5.8 TeV at the HL-LHC and 26.8 TeV at the FCC-hh.

4 The minimal left-right symmetric model

We now consider the TeV-scale LRSM based on the gauge group SU(2)$_L \times$ SU(2)$_R \times$ U(1)$_{B-L}$ [10–12]. Original aim of this model was to explain the asymmetric chiral structure of electroweak interactions in the SM. It was subsequently pointed out that it could account for the observed small neutrino masses via the type-I [13–17] and/or type-II [76–81]

---

[3]When the v_R scale changes from 5 TeV, the perturbative constraints on r_g in figure 3 will change accordingly from those given below eq. (3.3). However, this change is negligible for v_R up to 50 TeV.
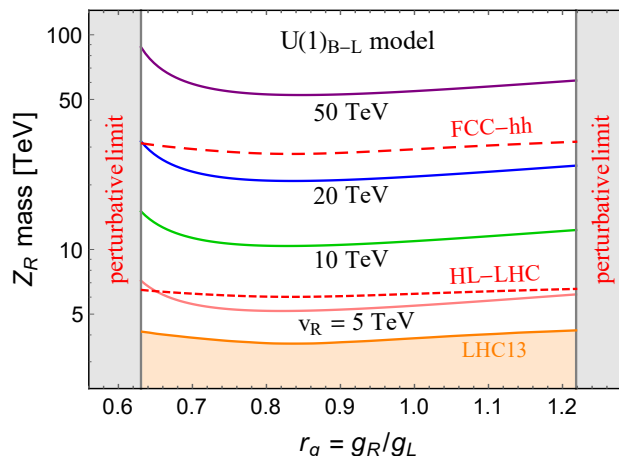
Figure 3. Current LHC13 constraints on Z_R mass in the $U(1)_{B-L}$ model (shaded orange) as function of $r_g = g_R/g_L$, and future prospects at the HL-LHC 14 TeV with an integrated luminosity of $3000\,\mathrm{fb}^{-1}$ (short-dashed red) and the 100 TeV collider FCC-hh with a luminosity of 30 ab^{-1} (long-dashed red). The vertical shaded regions are excluded by the perturbativity constraints given in eq. (3.3). The pink, green, blue and purple contours show the variation of the Z_R mass with respect to r_g, with the RH scale $v_R = 5, 10, 20, 50$ TeV, respectively.
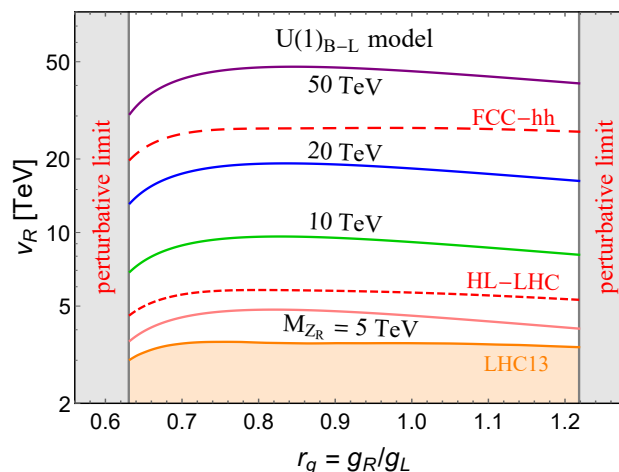

Figure 4. Current lower bound on the v_R scale in the $U(1)_{B-L}$ model, as functions of $r_g = g_R/g_L$, from the searches of Z_R in the dilepton channel at LHC 13 TeV (shaded orange), as well as the future limit from HL-LHC 14 TeV with an integrated luminosity of $3000\,\mathrm{fb}^{-1}$ (short-dashed red) and the 100 TeV collider FCC-hh with a luminosity of 30 ab^{-1} (long-dashed red). The vertical shaded regions are excluded by the perturbativity constraints given in eq. (3.3). The pink, green, blue and purple contours show the variation of v_R with respect to r_g, with the Z_R mass $M_{Z_R} = 5$, 10, 20, 50 TeV, respectively.

seesaw mechanisms. In the "canonical" version of LRSM, it is always assumed that the gauge coupling $g_R = g_L$ and the scalar content of the LRSM consists of one bidoublet Φ and the left-handed (Δ_L) and right-handed (Δ_R) triplets. As long as the RH scale v_R is at the few-TeV range, the values of g_R and g_{BL} and their RG running up to the GUT scale are al-

	$\mathrm{SU(2)}_L$	$\mathrm{SU(2)}_R$	$\mathrm{U(1)}_{B-L}$
$Q_L \equiv \begin{pmatrix} u_L \\ d_L \end{pmatrix}$	**2**	**1**	$\frac{1}{3}$
$Q_R \equiv \begin{pmatrix} u_R \\ d_R \end{pmatrix}$	**1**	**2**	$\frac{1}{3}$
$\psi_L \equiv \begin{pmatrix} \nu_L \\ e_L \end{pmatrix}$	**2**	**1**	-1
$\psi_R \equiv \begin{pmatrix} N \\ e_R \end{pmatrix}$	**1**	**2**	-1
$\Phi = \begin{pmatrix} \phi_1^0 & \phi_2^+ \\ \phi_1^- & \phi_2^0 \end{pmatrix}$	**2**	**2**	0
$\Delta_R = \begin{pmatrix} \frac{1}{\sqrt{2}}\Delta_R^+ & \Delta_R^{++} \\ \Delta_R^0 & -\frac{1}{\sqrt{2}}\Delta_R^+ \end{pmatrix}$	**1**	**3**	2

Table 3. Particle content of the minimal LRSM based on the gauge group $\mathrm{SU(2)}_L \times \mathrm{SU(2)}_R \times \mathrm{U(1)}_{B-L}$.

most fixed, at least at the one-loop level. However, the coupling g_R might be different from g_L, which generates very rich phenomenology in the LRSM, see e.g. [64, 68, 69, 82, 83]. Moreover, a free g_R not necessarily equal to g_L makes it possible to investigate the whole parameter space of perturbative constraints in the LRSM. In addition, the parity and $\mathrm{SU(2)}_R$ breaking scales might also be different such that the left-handed triplet Δ_L decouples from the TeV-scale physics [84]. This also helps to avoid the unacceptably large type-II seesaw contribution to the neutrino masses and/or fine-tuning in the scalar sector. Based on these arguments, we will not consider the Δ_L field in the low-energy LRSM. The matter content and the scalar fields in the minimal LRSM are collected in table 3. Three RHNs $N_{1,2,3}$ have been naturally introduced to form the RH lepton doublets ψ_R and accommodate the type-I seesaw mechanism. The perturbative constraints from the gauge and scalar sectors follow in the next two subsections.

4.1 Perturbativity constraints from the gauge sector

The perturbativity limits in the gauge sector are conceptually similar to the $\mathrm{U(1)}_{B-L}$ model in section 3; the difference is mainly due to the β-function coefficients, which in this case are given by

$$16\pi^2 \beta(g_R) = -\frac{7}{3}\,g_R^3\,, \tag{4.1}$$

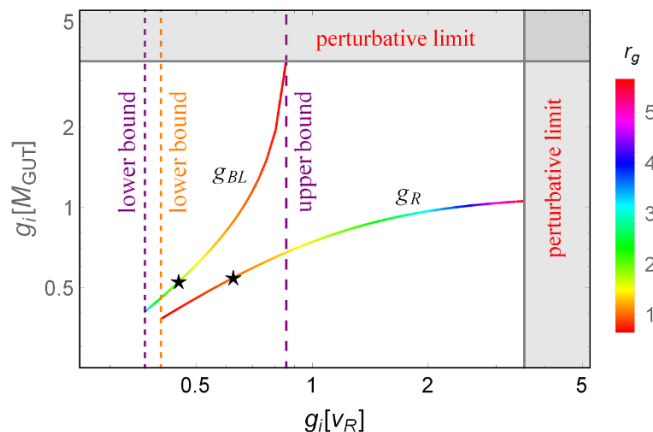$$16\pi^2 \beta(g_{BL}) = \frac{11}{3}\,g_{BL}^3\,. \tag{4.2}$$

Figure 5. Correlation of $g_{R,BL}(v_R)$ and $g_{R,BL}(M_{\rm GUT})$ in the minimal LRSM as functions of $r_g = g_R/g_L$ at the v_R scale (as shown by the color coding). The shaded regions are excluded by the perturbativity limits $g_{R,BL} < \sqrt{4\pi}$. The two stars correspond to the special case $g_R = g_L$ at the v_R scale. The vertical dotted and dashed lines respectively denote the lower and upper limits on the gauge couplings. Here we have chosen $v_R = 10\,{\rm TeV}$ and $M_{\rm GUT} = 10^{16}\,{\rm GeV}$.

Note the change in sign for $\beta(g_R)$, as compared to eq. (3.1), which is due to the non-Abelian nature of $SU(2)_R$. For completeness, we have also computed the two-loop RGEs using the code PyR@TE [85, 86] and list them in appendix A, although it turns out that the two-loop corrections change the results only by a few per cent, as compared to the one-loop results presented here.

As the RH scale $v_R = 5\,{\rm TeV}$ (chosen in section 3) is in tension with the stringent constraints from the scalar sector in LRSM (see section 4.2 and figure 8), we set $v_R = 10\,{\rm TeV}$ as an illustrative example to evaluate the perturbative constraints on the gauge couplings g_R and g_{BL}. In fact, as long as the v_R scale is at the ballpark of few-TeV, the changes in the running of g_R and g_{BL} are mainly due to the initial values of $g_{R,BL}$ at the v_R scale, and are negligibly small. As in the $U(1)_{B-L}$ model in section 3, the couplings g_R and g_{BL} are both functions of the ratio $r_g = g_R/g_L$. The correlations of $g_{R,BL}$ at the v_R scale and the GUT scale are presented in figure 5, as functions of r_g (as shown by the color coding). The two stars in figure 5 correspond to the special case $g_R = g_L$ at the v_R scale. As a result of non-Abelian nature of the $SU(2)_R$ group, g_R is asymptotically free, i.e. it becomes smaller at higher energy scales. Thus g_R could go up to the perturbativity limit of $\sqrt{4\pi}$ at the v_R scale (without considering the perturbativity limits from the scalar sector for the moment), which is very different from the $U(1)_{B-L}$ model, where the g_R value is much more restricted at the v_R scale [cf. figure 1]. The allowed ranges of the gauge couplings in the minimal LRSM are

$$0.406 < g_R < \sqrt{4\pi} \quad \text{and} \quad 0.369 < g_{BL} < 0.857, \quad \text{with} \quad 0.648 < r_g < 5.65 \qquad (4.3)$$

at the scale v_R, which is clearly shown in the correlation plot of g_R and g_{BL} in figure 6.

In the LRSM, the couplings of Z_R boson to the SM fermions and the heavy RHNs are the same as in the $U(1)_{B-L}$ model in section 3. Thus, the dilepton limits from current
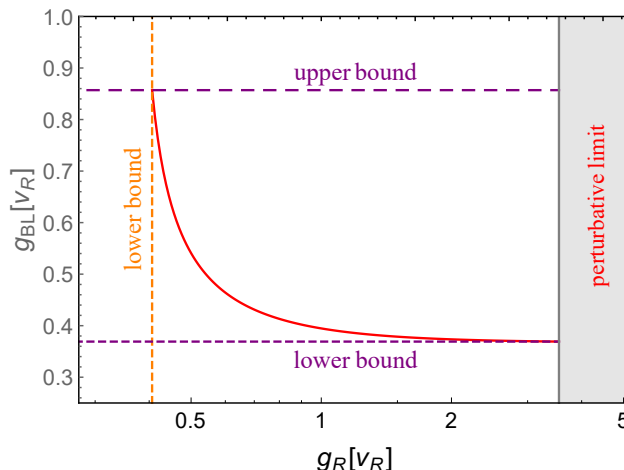
Figure 6. Correlation of g_R and g_{BL} in the minimal LRSM at the scale $v_R = 10\,\text{TeV}$ (red curve), along with the lower and upper bounds on the couplings $g_{R,\,BL}$, induced from the requirement of perturbativity up to the GUT scale. The shaded region is excluded by the perturbativity limit $g_R < \sqrt{4\pi}$.

LHC 13 TeV data [31, 32] and the prospects at the HL-LHC [74, 75] and future 100 TeV colliders [34, 75] are also the same as in U(1)$_{B-L}$ model, up to the different perturbative windows for the gauge couplings in eqs. (3.3) and (4.3), respectively. The current LHC 13 TeV dilepton constraints on the Z_R mass in the minimal LRSM and the future prospects are shown in the right panel of figure 7, along with the contours for $M_{Z_R}(r_g)$ with the RH scale $v_R = 5$, 10, 20 and 50 TeV. In the plot we have also shown the absolute theoretical lower bound on $r_g > \tan\theta_w$ from eq. (2.6) as the dashed vertical line, which is weaker than the "real" lower bound from perturbativity up to the GUT scale shown in figures 5 and 6 (the solid vertical gray line in figure 7). The scalar perturbativity limit shown in figure 7 will be discussed in section 4.2.

As for the limits on W_R boson in the LRSM, due to the Majorana nature of the heavy RHNs, the same-sign dilepton plus jets $pp \to W_R \to \ell^\pm N \to \ell^\pm \ell^\pm jj$ is the "smoking-gun" signal from the production and decay of the heavy W_R boson at hadron colliders [87]. The associated searches of W_R and RHN have been performed at LHC 13 TeV [29, 30]. To be concrete, we fix the RHN mass $M_N = 1\,\text{TeV}$; for such a benchmark scenario, the current LHC data requires that the W_R mass $M_{W_R} > 4.7\,\text{TeV}$ for $g_R = g_L$ [30]. If $g_R \neq g_L$, we have to re-evaluate the dependence of the production of W_R and the subsequent decays $W_R \to \ell^\pm N$ and $N \to \ell^\pm \ell\ell$ on the gauge coupling g_R.[4] Specifically,

- The production of W_R at hadron colliders is proportional to the W_R couplings to the SM quarks, i.e. $\sigma(pp \to W_R) \propto g_R^2$.

---

[4]The W_R boson might also decay into WZ and Wh, with the branching fractions depending largely on the VEV κ'/κ [83]. This does not affect the dependence of W_R production on the gauge coupling g_R. For simplicity, we have also neglected the effect of the heavy-light neutrino mixing on the W_R decay [88], since this mixing is severely constrained for TeV-scale LRSM with type-I seesaw [89].
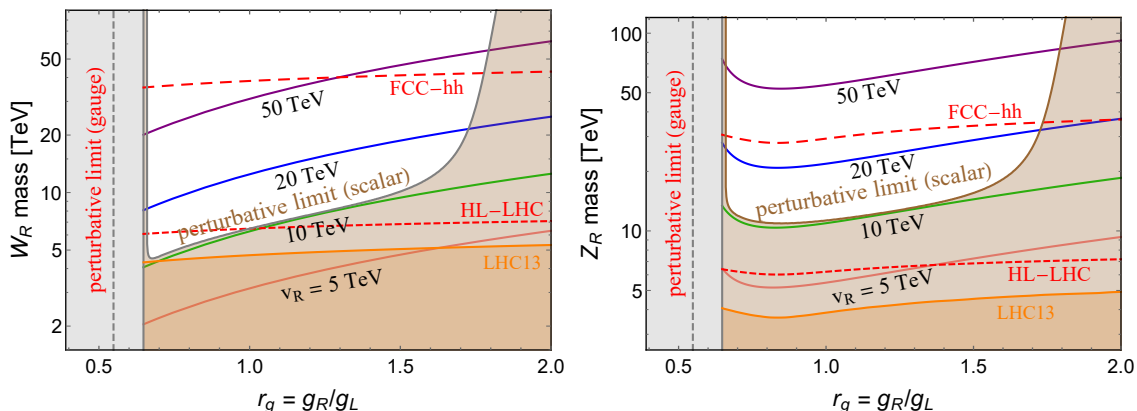
Figure 7. Current LHC13 constraints on the W_R (left) and Z_R (right) masses in the minimal LRSM (shaded orange) as function of $r_g = g_R/g_L$, and future prospects at the HL-LHC 14 TeV with an integrated luminosity of 3000 fb^{-1} (short-dashed red) and the 100 TeV collider FCC-hh with a luminosity of 30 ab^{-1} (long-dashed red). The pink, green, blue and purple lines are the W_R/Z_R mass with the RH scale $v_R = 5, 10, 20, 50$ TeV, respectively. The shaded gray and brown regions are excluded respectively by the perturbative constraints from the gauge and scalar sectors up to the GUT scale. The dashed vertical line corresponds to the absolute theoretical bound in eq. (2.6).

- The W_R boson decays predominately into the SM quarks and the charged leptons and heavy RHNs, i.e. $W_R \to \bar{q}_R q'_R$, $\ell_R N$. All the partial widths are proportional to g_R^2, but not the branching fraction BR($W_R \to \ell N$).

- In the limit of vanishing $W - W_R$ mixing and heavy-light neutrino mixing, $N \to \ell j j$ is the dominant decay mode (assuming N here is the lightest RHN), whose branching fraction does not depend on g_R.

In short, the g_R dependence is only relevant to the production $pp \to W_R$. For fixed W_R mass, we need only to rescale the production cross section $\sigma(pp \to W_R)$ by a factor of $r_g^2 = (g_R/g_L)^2$. The current LHC constraint on W_R mass is presented in the left panel of figure 7 as function of r_g, along with the contours of M_{W_R} for $v_R = 5, 10, 20$ and 50 TeV.

It is a good approximation in the minimal LRSM that the right-handed quark mixing matrix is identical to the CKM matrix in the SM, up to some unambiguous signs [90]. Then the W_R-mediated right-handed currents contributes to the $K_0 - \overline{K}_0$ and $B - \overline{B}$ mixings, leading to strong constraints on the W_R mass, $M_{W_R} \gtrsim 3$ TeV [42, 91–93]. This limit does not depend on the coupling g_R, as in the limit of $m_{K,B} \ll M_{W_R}$ the g_R dependence of W_R coupling to the SM quarks is canceled out by the dependence of g_R in the W boson propagator. The W_R contribution is effectively suppressed by $v_{\rm EW}^2/v_R^2$. As the quark flavor limits on W_R mass is significantly lower than that from the direct searches at the LHC for $r_g \gtrsim 0.65$, they are not shown in the left panel of figure 7. The W_R contributes also to neutrinoless double β-decays [94–102], which however depends on the masses of heavy RHNs and the doubly-charged scalars, and therefore, not included in figure 7.
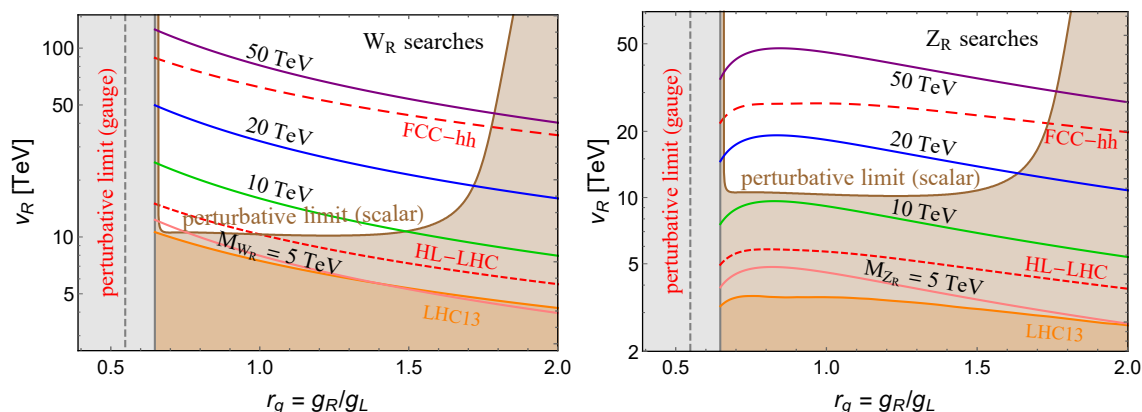
Figure 8. Lower bounds on the v_R scale in the minimal LRSM, as functions of r_g, from the direct searches of W_R and Z_R bosons at LHC 13 TeV (shaded orange), and future prospects at the HL-LHC 14 TeV with an integrated luminosity of $3000\,\mathrm{fb}^{-1}$ (short-dashed red) and the 100 TeV collider FCC-hh with a luminosity of 30 ab^{-1} (long-dashed red). The shaded gray regions are excluded by the perturbativity constraints up to the GUT scale, with the vertical dashed line corresponding to the absolute theoretical bound in eq. (2.6). The shaded brown regions are excluded by the perturbativity limits from the scalar sector, discussed in section 4.2.

The W_R could be probed up to 5.4 TeV at LHC 14 with a luminosity of $300\,\mathrm{fb}^{-1}$ [33, 103]. By rescaling the production cross section $\sigma(pp \to W_R)$ using CalcHEP [104], the W_R prospects could go up to 6.5 TeV for $g_R = g_L$ at the HL-LHC where the integrated luminosity is 10 times larger $(3000\,\mathrm{fb}^{-1})$. At future 100 TeV hadron colliders, for a relatively light RHN $M_N \ll M_{W_R}$, the decay products from the RHN tend to be highly-collimated and form fat jets. We adopt the analysis in ref. [36] where M_N/M_{W_R} was taken to be 0.1. Given a luminosity of 30 ab^{-1} at 100 TeV hadron colliders, the W_R mass could be probed up to 38.4 TeV with $g_R = g_L$. The projected sensitivity of W_R mass for a relatively low M_N at the HL-LHC and future 100 TeV collider FCC-hh could also be generalized to the case with $g_R \neq g_L$, which are depicted in the left panel of figure 7 respectively as the short-dashed and long-dashed red curves.

With the heavy gauge boson masses in the minimal LRSM

$$M_{W_R}^2 \simeq g_R^2 v_R^2, \quad M_{Z_R}^2 \simeq 2(g_R^2 + g_{BL}^2)v_R^2, \tag{4.4}$$

the current direct search limits of the W_R and Z_R boson at LHC 13 TeV and the future prospects at the HL-LHC and FCC-hh can be translated into limits on the v_R scale (as in the U(1)$_{B-L}$ model in section 3), which are presented in figure 8. For illustration purpose, we have also shown the contours of $M_{W_R}(M_{Z_R}) = 5$, 10, 20 and 50 TeV in the left (right) panel of figure 8, which are depicted respectively in pink, green, blue and purple. We find that the RH scale could be probed up to $\simeq 87$ TeV in the searches of W_R boson and ~ 25 TeV in the Z_R boson channel at the 100 TeV collider.

– 13 –

4.2 Perturbativity constraints from the scalar sector

The most general renormalizable scalar potential for the Φ and Δ_R fields is given by

$$
\begin{aligned}
\mathcal{V} = &-\mu_1^2 \operatorname{Tr}(\Phi^\dagger \Phi) - \mu_2^2 \left[\operatorname{Tr}(\tilde{\Phi}\Phi^\dagger) + \operatorname{Tr}(\tilde{\Phi}^\dagger \Phi) \right] - \mu_3^2 \operatorname{Tr}(\Delta_R \Delta_R^\dagger) \\
&+ \lambda_1 \left[\operatorname{Tr}(\Phi^\dagger \Phi) \right]^2 + \lambda_2 \left\{ \left[\operatorname{Tr}(\tilde{\Phi}\Phi^\dagger) \right]^2 + \left[\operatorname{Tr}(\tilde{\Phi}^\dagger \Phi) \right]^2 \right\} \\
&+ \lambda_3 \operatorname{Tr}(\tilde{\Phi}\Phi^\dagger)\operatorname{Tr}(\tilde{\Phi}^\dagger \Phi) + \lambda_4 \operatorname{Tr}(\Phi^\dagger \Phi) \left[\operatorname{Tr}(\tilde{\Phi}\Phi^\dagger) + \operatorname{Tr}(\tilde{\Phi}^\dagger \Phi) \right] \\
&+ \rho_1 \left[\operatorname{Tr}(\Delta_R \Delta_R^\dagger) \right]^2 + \rho_2 \operatorname{Tr}(\Delta_R \Delta_R)\operatorname{Tr}(\Delta_R^\dagger \Delta_R^\dagger) \\
&+ \alpha_1 \operatorname{Tr}(\Phi^\dagger \Phi)\operatorname{Tr}(\Delta_R \Delta_R^\dagger) + \left[\alpha_2 e^{i\delta_2}\operatorname{Tr}(\tilde{\Phi}^\dagger \Phi)\operatorname{Tr}(\Delta_R \Delta_R^\dagger) + \text{H.c.} \right] + \alpha_3 \operatorname{Tr}(\Phi^\dagger \Phi \Delta_R \Delta_R^\dagger).
\end{aligned}
\tag{4.5}
$$

Due to the LR symmetry, all the 12 parameters $\mu_{1,2,3}^2$, $\lambda_{1,2,3,4}$, $\rho_{1,2}$, $\alpha_{1,2,3}$ are real, and the only CP-violating phase is δ_2 associated with the coupling α_2, as explicitly shown in eq. (4.5).[5] The neutral component of the triplet develops a non-vanishing vacuum expectation value (VEV) $\langle \Delta_R^0 \rangle = v_R$, which breaks the $\mathrm{SU}(2)_R \times \mathrm{U}(1)_{B-L}$ down to the SM $\mathrm{U}(1)_Y$, and generates masses for the heavy scalars, the W_R and Z_R bosons and the RHNs. The bidoublet VEVs $\langle \phi_1^0 \rangle = \kappa$ and $\langle \phi_2^0 \rangle = \kappa'$ are responsible for the electroweak symmetry breaking. Neglecting the CP violation and up to the leading order in the small parameters $\epsilon = v_{\mathrm{EW}}/v_R$ and $\xi = \kappa'/\kappa$, the physical scalar masses are respectively [68]

$$
\begin{aligned}
M_h^2 &\simeq 4\lambda_1 v_{\mathrm{EW}}^2, & M_{H_1,\,A_1,\,H_1^\pm}^2 &\simeq \alpha_3 v_R^2, \\
M_{H_3}^2 &\simeq 4\rho_1 v_R^2, & M_{H_2^{\pm\pm}}^2 &\simeq 4\rho_2 v_R^2,
\end{aligned}
\tag{4.6}
$$

where h is the SM Higgs, H_1, A_1 and $H_1^\pm$ respectively the heavy CP-even and CP-odd neutral components and the singly-charged scalars from the bidoublet Φ, H_3 and $H_2^{\pm\pm}$ are the neutral and doubly-charged scalars from the triplet Δ_R, following the convention of ref. [68].

In the minimal LRSM, the heavy neutral scalars H_1 and A_1 have tree-level FCNC couplings to the SM quarks, which contribute to the $K_0 - \overline{K}_0$, $B_d - \overline{B}_d$ and $B_s - \overline{B}_d$ mixings. Thus their masses are tightly constrained by the high-precision flavor data, i.e. $M_H \gtrsim 10 \,\mathrm{TeV}$ [41–43]. For a few-TeV scale v_R, this implies that the quartic coupling $\alpha_3 \simeq M_{H_1}^2/v_R^2$ is pretty large, typically of order one. The RG running of the quartic couplings in eq. (4.5) are all entangled together, and a large α_3 is the main reason why the LRSM could easily hit a Landau pole at an energy scale that is much lower than the GUT scale [105–108]. This could be alleviated if the v_R scale is higher and the coupling α_3 gets smaller. Therefore, the perturbativity of the quartic couplings in eq. (4.5) up to the GUT scale could set a lower bound on the v_R scale, assuming there is no intermediate scales or particles in between v_R and the GUT scale.

---

[5]This potential stems from the full LRSM at a higher energy scale in presence of the left-handed triplet Δ_L. At the high scale, all but one of the couplings are real. At low scales there will be small phases in some couplings induced by radiative renormalization group effects. We ignore these small phases. Our main conclusions are not affected by this.

A thorough analysis of the RG running of all the quartic couplings in eq. (4.5) is rather complicated and it obfuscates the perturbativity limits on the v_R scale. While some of the quartic couplings could be tuned very small at the v_R scale as they only induce mixings among the scalars such as $\alpha_{1,2}$ [68], there are only four quartic couplings, i.e. the λ_1, α_3, ρ_1 and ρ_2 appearing in eq. (4.6), that are responsible for the scalar masses at the tree level. Therefore, for the purpose of perturbativity limits in the scalar sector, we consider a simple scenario with only these four non-vanishing quartic couplings λ_1, α_3, ρ_1 and ρ_2 at the v_R scale. In particular, we set the scalar masses to the following benchmark values:

$$M_h = 125\,\text{GeV}\,, \qquad\qquad M_{H_1,\,A_1,\,H_1^\pm} = 10\,\text{TeV}\,,$$
$$M_{H_3} = 100\,\text{GeV}\,, \qquad\qquad M_{H_2^{\pm\pm}} = 1\,\text{TeV}\,, \qquad (4.7)$$

from which one could obtain the values of λ_1, α_3, ρ_1 and ρ_2 by using eq. (4.6). All other quartic couplings $\lambda_{2,3,4}$, $\alpha_{1,2}$ are set to zero, and this corresponds to the limits without any tree-level scalar mixing at the v_R scale. In the limit of vanishing mixing between h and H_1, the neutral scalar H_3 from the triplet Δ_R is hadrophobic and the experimental constraints on H_3 are rather weak [70, 109]. Thus we have set H_3 to be light, at the 100 GeV scale, in eq. (4.7). The smoking-gun signal of a doubly-charged scalar is the same-sign dilepton pairs $H_2^{\pm\pm} \to \ell_\alpha^\pm \ell_\beta^\pm$ with $\alpha,\,\beta = e,\,\mu,\,\tau$, which is almost background free. The current most stringent limits are from the LHC 13 TeV data [110, 111], which requires that $M_{H_2^{\pm\pm}} \gtrsim (271-760)\,\text{GeV}$, depending largely on the charged lepton flavors involved [112]. To be concrete, we have set the doubly-charged scalar mass at 1 TeV in eq. (4.7), which easily satisfies the current LHC constraints. As for the bidoublet masses $M_{H_1,\,A_1,\,H_1^\pm}$, we have taken the minimum possible value allowed by FCNC constraints [42], whereas for the SM Higgs, we have taken the current best-fit value [113].

All the RGEs for the gauge couplings $g_{L,\,R,\,BL}$ and the quartic couplings in the potential in eq. (4.5) are collected in appendix A up to the two-loop level. To be self-consistent, we include also the RGE for the dominant Yukawa coupling h_t that is responsible for generation of the top quark mass at the electroweak scale. The Yukawa couplings for the bottom and tauon are comparatively much smaller and are neglected here. For a RH scale $v_R \gtrsim 10\,\text{TeV}$, the Yukawa coupling f_R of Δ_R to the lepton doublets are also small if the masses of the three RHNs $M_N \simeq \text{TeV}$. For simplicity, the f_R terms in the β-functions are also neglected. See appendix A for more details.

Given the scalar masses in eq. (4.7), all the β-functions for the quartic couplings in eq. (A.5) to (A.13) are dominated by the α_3 terms if the RH scale v_R is not too much higher than the TeV scale, i.e.

$$16\pi^2 \beta(\lambda_1) = \frac{5}{4}\alpha_3^2 + \frac{3}{8}\left(3g_L^4 + 2g_L^2 g_R^2 + 3g_R^4\right) - 6h_t^4 + \cdots\,, \qquad (4.8)$$

where the dots stand for the subleading terms. For a few-TeV v_R and $\alpha_3 \gtrsim \mathcal{O}(1)$, the quartic couplings rapidly blow up before reaching the GUT scale [105–108]. An explicit example is shown in the two upper panels of figure 9, with $r_g = g_R/g_L = 1.1$ and $v_R = 6\,\text{TeV}$, where the quartic couplings become non-perturbative at $\sim 10^7\,\text{GeV}$. When the RH scale v_R is higher, for a fixed mass $M_{H_1} = 10\,\text{TeV}$, the coupling $\alpha_3 \simeq M_{H_1}^2/v_R^2$ is significantly
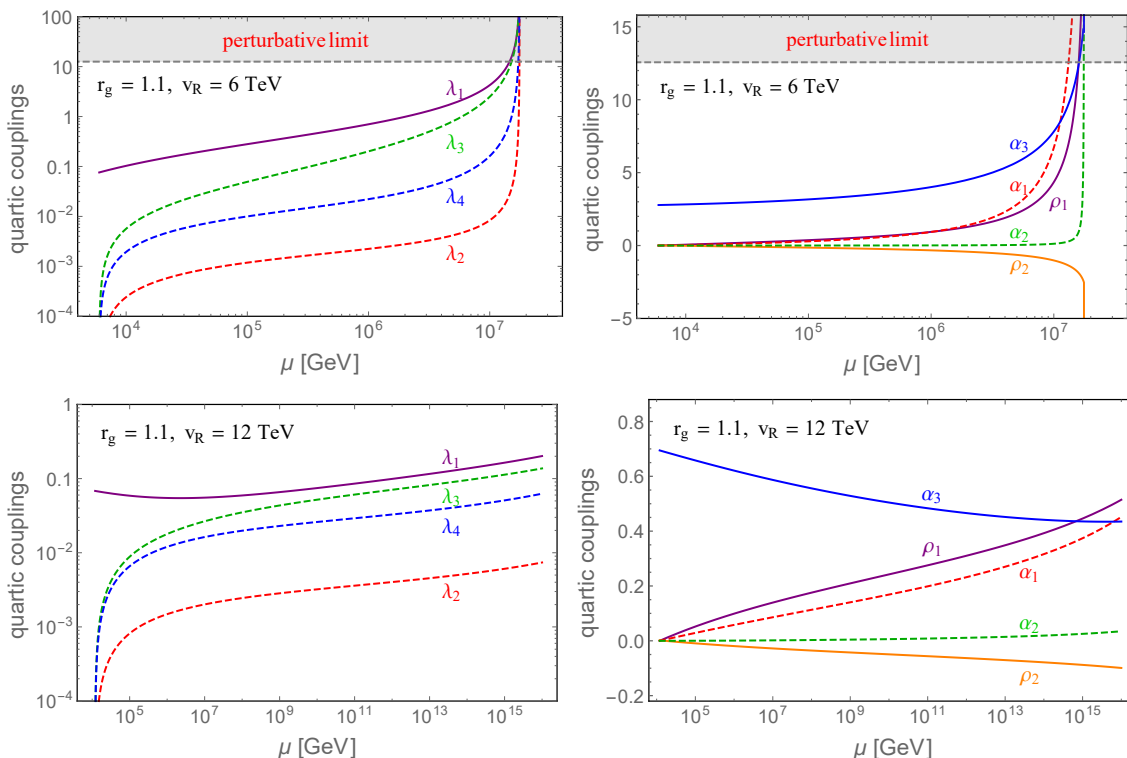
Figure 9. RG running of the quartic couplings $\lambda_{1,2,3,4}$ (left), and $\rho_{1,2}$, $\alpha_{1,2,3}$ (right) in the scalar potential eq. (4.5) of minimal LRSM from v_R up to the GUT scale, with $r_g = 1.1$ and $v_R = 6\,\text{TeV}$ (upper panels), $v_R = 12\,\text{TeV}$ (lower panels).

smaller. As a result, in a large region of the parameter space, all the quartic couplings are perturbative up to the GUT scale, as exemplified in the two lower panels of figure 9 with $r_g = g_R/g_L = 1.1$ and $v_R = 12\,\text{TeV}$. In both examples, the bounded-from-below conditions in the scalar sector are respected [107, 114]:[6]

$$\lambda_1 \geq 0\,, \quad \rho_1 \geq 0\,, \quad \rho_1 + \rho_2 \geq 0\,, \quad \rho_1 + 2\rho_2 \geq 0\,. \tag{4.9}$$

One should note that the g_R and g_{BL} terms in the β-functions in eqs. (A.5) to (A.13) might be unacceptably large. Thus the perturbativity limits in the scalar sector depend also on the gauge couplings g_R and g_{BL}, or equivalently the ratio $r_g = g_R/g_L$. As seen in eq. (4.8), when $g_R \gtrsim \mathcal{O}(1)$ [or $g_{BL} \gtrsim \mathcal{O}(1)$], the constraints on the v_R scale and α_3 tend to be more stringent. The r_g-dependent scalar perturbativity constraints on v_R are shown in figure 8 as the shaded brown regions. Numerically, we find the requirement in the minimal LRSM that

$$v_R \gtrsim 10\,\text{TeV} \quad \text{for} \quad 0.65 \lesssim r_g \lesssim 1.6\,, \tag{4.10}$$

which makes the perturbativity constraints very stringent in the gauge sector (see figures 5 and 6). The quartic couplings blow up very quickly when r_g is out of this range unless v_R is much higher than $10\,\text{TeV}$, as $g_R \gtrsim \mathcal{O}(1)$ or $g_{BL} \gtrsim \mathcal{O}(1)$.

---

[6]More generic vacuum stability criteria can be found, e.g., in ref. [115].

collider	W_R searches		Z_R searches	
	M_{W_R} [TeV]	v_R [TeV]	M_{Z_R} [TeV]	v_R [TeV]
LHC13	–	–	–	–
HL-LHC	$[6.09, 6.47]$	$[10.3, 14.8]$	–	–
FCC-hh	$[35.6, 42.2]$	$[38.3, 87.5]$	$[27.9, 35.4]$	$[21.8, 26.8]$

Table 4. Lower bounds on the W_R and Z_R boson masses and the corresponding v_R scale in the minimal LRSM from the current LHC13 data [30–32] and the prospects at the HL-LHC 14 TeV with an integrated luminosity of $3000\,\text{fb}^{-1}$ [33, 74, 75] and future 100 TeV collider FCC-hh with a luminosity of 30 ab^{-1} [34, 36, 75], with both the gauge and scalar perturbativity limits up to the GUT scale taken into consideration. The range in each case corresponds to the allowed range of r_g from perturbativity constraints, as given in figures 7 and 8. The missing entries mean that the corresponding maximum experimental reach has been excluded by the scalar perturbativity constraints. See text for more details.

It is remarkable that the perturbativity constraints from the scalar sector supersede the current LHC constraints on the W_R and Z_R bosons in the minimal LRSM, and even the projected Z_R sensitivity at the HL-LHC, leaving only a very narrow window for W_R, as shown in figure 7. Fortunately, future 100 TeV colliders could probe a much larger parameter space. All the numerical ranges of the maximum W_R and Z_R mass reach and the corresponding v_R scales at future hadron colliders are collected in table 4, with both the gauge and scalar perturbativity constraints taken into consideration. Finding a heavy W_R and/or Z_R boson at the HL-LHC, would have strong implications for the interpretation in the minimal LRSM. For instance, if a Z_R boson was to be found at the LHC, then it does not belong to the minimal LRSM. It could still be accommodated in the LRSM framework by introducing some exotic particles or an intermediate scale, e.g. at $\sim 10^6\,\text{GeV}$, to the minimal LRSM to keep all the gauge, Yukawa and quartic couplings perturbative up to the GUT scale.

It should be emphasized that the perturbative constraints on the W_R and Z_R masses and the v_R scale from the scalar sector shown in figures 7 and 8 are based on the assumptions of the scalar masses in eq. (4.7) and the vanishing quartic couplings $\lambda_{2,3,4}$, $\alpha_{1,2}$. In light of the stringent flavor constraints on the bidoublet scalars H_1, A_1 and $H_1^{\pm}$, the dilepton constraints on the doubly-charged scalar $H_2^{\pm\pm}$ and the flavor constraints on the neutral scalar H_3, the masses in eq. (4.7) are almost the most optimistic values allowed by the current data that could give us the most conservative perturbativity constraints. If the BSM Higgs masses get larger (especially in the bidoublet sector), the corresponding quartic couplings α_3, ρ_1 and ρ_2 will be accordingly enhanced by M^2/v_R^2 at the v_R scale (with M standing for the generic BSM scalar mass), and the scalar perturbativity limits on the v_R scale would be more stringent. Furthermore, if the couplings $\lambda_{2,3,4}$, $\alpha_{1,2}$ are not zero at the v_R scale, the quartic couplings tend to hit the Landau pole at a lower scale.

We have also checked also the two-loop corrections to the scalar perturbativity limits by deriving all the two-loop RGEs using the code PyR@TE [85, 86], as collected in eqs. (A.1)

to (A.14). It turns out that the two-loop corrections only amount to less than 3% different for the scalar perturbativity limits on v_R and the heavy gauge boson masses, as compared to the one-loop results presented in this section.

In the limit of small scalar mixing, just as we have assumed above, λ_1 can be identified as the SM quartic coupling. As a byproduct, the extra scalars in the LRSM contribute positively to the $\beta(\lambda_1)$ in eq. (A.5) in a larger region of parameter space, which helps to stabilize the SM vacuum up to the GUT scale or even up to the Planck scale. The full analysis of the stability of the scalar potential is beyond the main scope of this paper. See ref. [114] for a recent analysis in this direction.

5 Conclusion

In conclusion, we find that in the extensions of the electroweak gauge group to either $\mathrm{SU}(2)_L \times \mathrm{U}(1)_{I_{3R}} \times \mathrm{U}(1)_{B-L}$ or the left-right symmetric group $\mathrm{SU}(2)_L \times \mathrm{SU}(2)_R \times \mathrm{U}(1)_{B-L}$, both of which contribute to the electric charge, there are strong limits on the new gauge couplings g_R and g_{BL} from the requirement that the couplings remain perturbative till the GUT scale. We obtain those limits for the minimal versions of these models and study their implications for collider phenomenology. We find in particular that the ratio $r_g \equiv g_R/g_L$, or effectively the gauge couplings g_R and g_{BL}, are limited to a very narrow range at the TeV scale, as seen in figures 2 and 6. Inclusion of the scalar sector in the minimal LRSM implies that the RH symmetry breaking scale in LRSM must have a lower bound of about 10 TeV for a limited coupling range $0.65 \lesssim r_g \lesssim 1.6$. The gauge (and scalar) perturbative constraints have rich implications for the searches of Z_R (and W_R) bosons in these models at the HL-LHC and future 100 TeV colliders. All the direct search constraints on the W_R and Z_R masses from LHC 13 TeV, as well as the future prospects at HL-LHC and 100 TeV colliders, depend on the BSM gauge couplings g_R and g_{BL} (or effectively the ratio r_g). All the Z_R (and W_R) mass ranges and the corresponding v_R scales are collected in figures 3, 4 and table 2 for the $\mathrm{U}(1)_{B-L}$ model, and figures 7, 8 and table 4 for the LRSM. One of the most striking results we find is that the perturbativity constraints already exclude the possibility of finding the Z_R boson belonging to the minimal LRSM at the HL-LHC, and leave only a narrow window for the W_R boson. We hope this serves as an additional motivation for the 100 TeV collider, where a much broader parameter space can be probed.

A Two-loop RGEs for the minimal LRSM

Here we list the β-functions for the gauge couplings $g_{S,L,R,BL}$, the quartic couplings $\lambda_{1,2,3,4}$, $\rho_{1,2}$ and $\alpha_{1,2,3}$ in the scalar potential (4.5) and the Yukawa coupling h_t in the minimal LRSM up to two-loop level, which are obtained by using PyR@TE [85, 86]:[7]

$$\beta(g_S) = \frac{1}{16\pi^2}\left[-7\,g_S^3\right] + \frac{1}{(16\pi^2)^2}\left[\frac{1}{6}g_S^3\left(2g_{BL}^2 + 3\left(9g_L^2 + 9g_R^2 - 52g_S^2 - 8h_t^2\right)\right)\right], \quad (A.1)$$

$$\beta(g_L) = \frac{1}{16\pi^2}\left[-3\,g_L^3\right] + \frac{1}{(16\pi^2)^2}\left[g_L^3\left(g_{BL}^2 + 3\left(g_R^2 + 4g_S^2 - h_t^2\right) + 8g_L^2\right)\right], \quad (A.2)$$

$$\beta(g_R) = \frac{1}{16\pi^2}\left[-\frac{7}{3}\,g_R^3\right] + \frac{1}{(16\pi^2)^2}\left[\frac{1}{3}g_R^3\left(27g_{BL}^2 + 9g_L^2 + 80g_R^2 + 36g_S^2 - 9h_t^2\right)\right], \quad (A.3)$$

$$\beta(g_{BL}) = \frac{1}{16\pi^2}\left[\frac{11}{3}\,g_{BL}^3\right] + \frac{1}{(16\pi^2)^2}\left[\frac{1}{9}g_{BL}^3\left(122g_{BL}^2 + 3\left(9g_L^2 + 81g_R^2 + 8g_S^2 - 2h_t^2\right)\right)\right], \quad (A.4)$$

$$\begin{aligned}
\beta(\lambda_1) = &\frac{1}{16\pi^2}\Bigg[\frac{3}{8}\left(3g_L^4 + 2g_L^2 g_R^2 + 3g_R^4\right) + 16(2\lambda_1^2 + 4\lambda_2^2 + \lambda_3^2 + 3\lambda_4^2)\\
&+ 3\alpha_1^2 + 3\alpha_1\alpha_3 + \frac{5}{4}\alpha_3^2 - 6h_t^4 - 9\lambda_1\left(g_L^2 + g_R^2\right) + 16\lambda_1\lambda_3 + 12\lambda_1 h_t^2\Bigg]\\
&+ \frac{1}{(16\pi^2)^2}\Bigg[\frac{291g_L^6}{16} + \frac{235g_R^6}{16} + g_L^4\left(-\frac{191g_R^2}{16} - \frac{9h_t^2}{4} + \frac{69\lambda_1}{8} + 15\lambda_3\right)\\
&+ g_{BL}^2\left(24\alpha_1^2 + 10\alpha_3^2 + 24\alpha_1\alpha_3 + \frac{5}{3}\lambda_1 h_t^2 - \frac{2}{3}h_t^4\right)\\
&- \frac{1}{48}g_L^2\left(12g_R^2\left(30h_t^2 - 69\lambda_1 - 56\lambda_3\right) + 629g_R^4\right.\\
&\left.- 72\left(15\lambda_1 h_t^2 + 8\left(13\lambda_1^2 + 8\lambda_3\lambda_1 + 4\lambda_3^2 + 18\lambda_4^2\right)\right)\right)\\
&+ g_R^4\left(30\alpha_1 + 15\alpha_3 - \frac{9h_t^2}{4} + \frac{157\lambda_1}{8} + 15\lambda_3\right)\\
&+ g_R^2\left(48\alpha_1^2 + 17\alpha_3^2 + 48\alpha_1\alpha_3 + \frac{45}{2}\lambda_1 h_t^2 + 156\lambda_1^2 + 48\lambda_3^2 + 216\lambda_4^2 + 96\lambda_1\lambda_3\right)\\
&- 30\alpha_1^2\lambda_1 - 24\alpha_2^2\lambda_1 - \frac{29}{2}\alpha_3^2\lambda_1 - 30\alpha_1\alpha_3\lambda_1 - 192\alpha_2^2\lambda_2 - 96\alpha_2^2\lambda_3 - 144\alpha_1\alpha_2\lambda_4\\
&- 72\alpha_2\alpha_3\lambda_4 - 12\alpha_1^3 - \frac{13\alpha_3^3}{2} - 48\alpha_1\alpha_2^2 - 19\alpha_1\alpha_3^2 - 18\alpha_1^2\alpha_3 - 24\alpha_2^2\alpha_3\\
&+ 16g_S^2 h_t^2\left(5\lambda_1 - 2h_t^2\right) + 36h_t^6 - 12\lambda_1 h_t^4 - 96h_t^2\left(2\lambda_1^2 + 4\lambda_2^2 + \lambda_3^2 + 3\lambda_4^2 + \lambda_1\lambda_3\right)\\
&- 456\lambda_1^3 - 384\lambda_3^3 - 3456\lambda_1\lambda_2^2 - 704\lambda_1\lambda_3^2 - 2208\lambda_1\lambda_4^2 - 3328\lambda_2\lambda_4^2\\
&- 1792\lambda_3\lambda_4^2 - 352\lambda_1^2\lambda_3 - 5632\lambda_2^2\lambda_3\Bigg], \quad (A.5)
\end{aligned}$$

---

[7]Note that some of the one-loop coefficients obtained here are different from those in refs. [105, 106]. In particular, the coefficient for g_R in these references is $-5/2$, while, with the same matter and scalar fields that contribute to the running of g_R, we found it is $-7/3$.

$$\beta(\lambda_2) = \frac{1}{16\pi^2}\left[12\lambda_4^2 + 3\alpha_2^2 + \frac{3}{16}h_t^4 - 9\lambda_2(g_L^2 + g_R^2) + 24\lambda_2(\lambda_1 + 2\lambda_3) + 12\lambda_2 h_t^2\right]$$

$$+ \frac{1}{(16\pi^2)^2}\left[-24\alpha_2^2\lambda_1 - 30\alpha_1^2\lambda_2 + 24\alpha_2^2\lambda_2 + \frac{3}{2}\alpha_3^2\lambda_2 - 30\alpha_1\alpha_3\lambda_2 - 24\alpha_2^2\lambda_3\right.$$

$$-36\alpha_1\alpha_2\lambda_4 - 18\alpha_2\alpha_3\lambda_4 - 24\alpha_1\alpha_2^2 - 12\alpha_2^2\alpha_3 + 24\alpha_2^2 g_{BL}^2 + \frac{5}{3}\lambda_2 g_{BL}^2 h_t^2$$

$$+ g_L^2\left(\frac{57}{4}\lambda_2 g_R^2 + \frac{45}{2}\lambda_2 h_t^2 - \frac{9h_t^4}{32} + 54\lambda_4^2 + 72\lambda_1\lambda_2 + 288\lambda_2\lambda_3\right)$$

$$+ g_R^2\left(48\alpha_2^2 + \frac{45}{2}\lambda_2 h_t^2 - \frac{9h_t^4}{32} + 54\lambda_4^2 + 72\lambda_1\lambda_2 + 288\lambda_2\lambda_3\right)$$

$$+ 80\lambda_2 g_S^2 h_t^2 - \frac{231}{8}\lambda_2 g_L^4 - \frac{143}{8}\lambda_2 g_R^4 - 72\lambda_4^2 h_t^2 - 36\lambda_2 h_t^4$$

$$-144\lambda_1\lambda_2 h_t^2 - 288\lambda_2\lambda_3 h_t^2 + 384\lambda_2^3 - 512\lambda_2\lambda_3^2 - 432\lambda_1\lambda_4^2$$

$$\left. -1248\lambda_2\lambda_4^2 - 480\lambda_3\lambda_4^2 - 488\lambda_1^2\lambda_2 - 1312\lambda_1\lambda_2\lambda_3\right], \tag{A.6}$$

$$\beta(\lambda_3) = \frac{1}{16\pi^2}\left[\frac{27}{8}h_t^4 + 6\alpha_2^2 - \frac{1}{2}\alpha_3^2 + \frac{3}{2}g_L^2 g_R^2 - 9\lambda_3(g_L^2 + g_R^2)\right.$$

$$\left. +12\lambda_3 h_t^2 + 8(3\lambda_1\lambda_3 + 16\lambda_2^2 + 2\lambda_3^2 + 3\lambda_4^2)\right]$$

$$+ \frac{1}{(16\pi^2)^2}\left[\frac{291g_L^6}{32} - \frac{1}{32}\left(415g_R^2 + 6\left(6h_t^2 - 23\lambda_1 - 308\lambda_2 + 114\lambda_3\right)\right)g_L^4\right.$$

$$- \frac{1}{96}\left(1525g_R^4 + 12\left(30h_t^2 - 165\lambda_1 + 228\lambda_2 - 298\lambda_3\right)g_R^2\right.$$

$$-72\left(15\left(\lambda_1 - 4\lambda_2 + 2\lambda_3\right)h_t^2 + 8\left(13\lambda_1^2 - 4\left(6\lambda_2 - 5\lambda_3\right)\lambda_1\right.\right.$$

$$\left.\left.\left. +2\left(72\lambda_2^2 - 48\lambda_3\lambda_2 + 8\lambda_3^2 + 9\lambda_4^2\right)\right)\right)\right)g_L^2$$

$$+ \frac{235g_R^6}{32} + 6h_t^6 - 6\alpha_1^3 - \frac{5\alpha_3^3}{4} - 228\lambda_1^3 - 768\lambda_2^3 - 192\lambda_3^3 + 12g_{BL}^2\alpha_1^2$$

$$-24\alpha_1\alpha_2^2 + g_{BL}^2\alpha_3^2 - \frac{11}{2}\alpha_1\alpha_3^2 - 96h_t^2\lambda_1^2 - 960h_t^2\lambda_2^2$$

$$-4800\lambda_1\lambda_2^2 - 144h_t^2\lambda_3^2 - 896\lambda_1\lambda_3^2 + 1024\lambda_2\lambda_3^2 - 36\alpha_2\alpha_3\lambda_4$$

$$-144h_t^2\lambda_4^2 - 1104\lambda_1\lambda_4^2 - 1216\lambda_2\lambda_4^2 - 1120\lambda_3\lambda_4^2 - 9\alpha_1^2\alpha_3$$

$$-12\alpha_2^2\alpha_3 + 12g_{BL}^2\alpha_1\alpha_3 - 18h_t^4\lambda_1 + \frac{5}{6}g_{BL}^2 h_t^2\lambda_1 - 72\alpha_1\alpha_2\lambda_4$$

$$+40g_S^2 h_t^2\lambda_1 - 15\alpha_1^2\lambda_1 - 12\alpha_2^2\lambda_1 - \frac{13}{4}\alpha_3^2\lambda_1 - 15\alpha_1\alpha_3\lambda_1$$

$$+72h_t^4\lambda_2 - \frac{10}{3}g_{BL}^2 h_t^2\lambda_2 - 160g_S^2 h_t^2\lambda_2 + 60\alpha_1^2\lambda_2 - 240\alpha_2^2\lambda_2$$

$$-3\alpha_3^2\lambda_2 + 976\lambda_1^2\lambda_2 + 60\alpha_1\alpha_3\lambda_2 + 288h_t^2\lambda_1\lambda_2 - 60h_t^4\lambda_3$$

$$+\frac{5}{3}g_{BL}^2 h_t^2\lambda_3 + 80g_S^2 h_t^2\lambda_3 - 30\alpha_1^2\lambda_3 + 24\alpha_2^2\lambda_3 + \frac{3}{2}\alpha_3^2\lambda_3 - 664\lambda_1^2\lambda_3$$

$$-4480\lambda_2^2\lambda_3 - 30\alpha_1\alpha_3\lambda_3 - 192h_t^2\lambda_1\lambda_3 + 576h_t^2\lambda_2\lambda_3 + 2624\lambda_1\lambda_2\lambda_3$$

$$-\frac{1}{16}g_R^4\left(18h_t^2 - 240\alpha_1 - 120\alpha_3 - 157\lambda_1 - 572\lambda_2 + 166\lambda_3\right)$$

$$+ g_R^2 \left(\frac{45}{4} \lambda_1 h_t^2 - 45\lambda_2 h_t^2 + \frac{45}{2} \lambda_3 h_t^2 + 24\alpha_1^2 + \frac{7\alpha_3^2}{2} + 78\lambda_1^2 + 864\lambda_2^2 \right.$$

$$\left. \left. + 96\lambda_3^2 + 108\lambda_4^2 + 24\alpha_1\alpha_3 - 144\lambda_1\lambda_2 + 120\lambda_1\lambda_3 - 576\lambda_2\lambda_3 \right) \right], \tag{A.7}$$

$$\beta(\lambda_4) = \frac{1}{16\pi^2} \left[3\alpha_2(2\alpha_1 + \alpha_3) + \frac{3}{2} h_t^4 - 9\lambda_4(g_L^2 + g_R^2) + 48(\lambda_1 + 2\lambda_2 + \lambda_3)\lambda_4 + 12\lambda_4 h_t^2 \right]$$

$$+ \frac{1}{(16\pi^2)^2} \left[-72\alpha_1\alpha_2\lambda_1 - 36\alpha_2\alpha_3\lambda_1 - 144\alpha_1\alpha_2\lambda_2 - 72\alpha_2\alpha_3\lambda_2 - 72\alpha_1\alpha_2\lambda_3 \right.$$

$$- 36\alpha_2\alpha_3\lambda_3 - 30\alpha_1^2\lambda_4 - 120\alpha_2^2\lambda_4 - \frac{9}{2}\alpha_3^2\lambda_4 - 30\alpha_1\alpha_3\lambda_4 - 48\alpha_2^3$$

$$- 15\alpha_2\alpha_3^2 - 36\alpha_1^2\alpha_2 - 36\alpha_1\alpha_2\alpha_3 + g_{BL}^2 \left(48\alpha_1\alpha_2 + 24\alpha_2\alpha_3 + \frac{5}{3}\lambda_4 h_t^2 \right)$$

$$+ \frac{3}{4} g_R^2 \left(128\alpha_1\alpha_2 + 64\alpha_3\alpha_2 + 3\lambda_4 \left(13g_L^2 + 2 \left(5h_t^2 + 48\left(\lambda_1 + 2\lambda_2 + \lambda_3\right) \right) \right) \right)$$

$$+ \frac{45}{2} \lambda_4 g_L^2 h_t^2 + 80\lambda_4 g_S^2 h_t^2 - \frac{51}{8} \lambda_4 g_L^4 + 216\lambda_1\lambda_4 g_L^2 + 432\lambda_2\lambda_4 g_L^2 + 216\lambda_3\lambda_4 g_L^2$$

$$+ \left(30\alpha_2 + \frac{37\lambda_4}{8} \right) g_R^4 - 36\lambda_4 h_t^4 - 288\lambda_1\lambda_4 h_t^2 - 576\lambda_2\lambda_4 h_t^2 - 288\lambda_3\lambda_4 h_t^2$$

$$- 1248\lambda_4^3 - 1064\lambda_1^2\lambda_4 - 4992\lambda_2^2\lambda_4 - 1088\lambda_3^2\lambda_4$$

$$\left. - 3456\lambda_1\lambda_2\lambda_4 - 1888\lambda_1\lambda_3\lambda_4 - 3840\lambda_2\lambda_3\lambda_4 \right], \tag{A.8}$$

$$\beta(\rho_1) = \frac{1}{16\pi^2} \left[3 \left(3g_R^4 + 4g_R^2 g_{BL}^2 + 2g_{BL}^4 \right) + 2 \left(2\alpha_1^2 + 8\alpha_2^2 + 2\alpha_1\alpha_3 + \alpha_3^2 \right) \right.$$

$$\left. + 28\rho_1^2 + 16\rho_2^2 - 12\rho_1 \left(2g_R^2 + g_{BL}^2 \right) + 16\rho_1\rho_2 \right]$$

$$+ \frac{1}{(16\pi^2)^2} \left[-\frac{2}{3} \left(2g_{BL}^4 \left(233g_R^2 - 170\rho_1 - 60\rho_2 \right) + 4g_{BL}^2 \left(3 \left(-17\rho_1 + 20\rho_2 \right) g_R^2 \right. \right. \right.$$

$$+ 118g_R^4 - 6 \left(11\rho_1^2 + 4\left(2\rho_2 \right) \rho_1 + 8\rho_2^2 \right) \right) + 196g_{BL}^6$$

$$+ 3 \left(20\alpha_1^2\rho_1 + 20\alpha_3\alpha_1\rho_1 + 80\alpha_2^2\rho_1 + 11\alpha_3^2\rho_1 + 8\alpha_1^3 + 12\alpha_3\alpha_1^2 \right.$$

$$+ 96\alpha_2^2\alpha_1 + 14\alpha_3^2\alpha_1 + 5\alpha_3^3 + 48\alpha_2^2\alpha_3 - 6 \left(2\alpha_1^2 + 2\alpha_3\alpha_1 + 8\alpha_2^2 + \alpha_3^2 \right) g_L^2$$

$$+ 6 \left(2\alpha_1^2 + 2\alpha_3\alpha_1 + 8\alpha_2^2 + \alpha_3^2 \right) h_t^2 + 192\rho_1^3 + 160\rho_2^3 + 312\rho_1\rho_2^2 + 176\rho_1^2\rho_2 \right)$$

$$- 2 \left(30\alpha_1 + 15\alpha_3 + 154\rho_1 + 96\rho_2 \right) g_R^4 - 3 \left(12\alpha_1^2 + 12\alpha_3\alpha_1 + 48\alpha_2^2 \right.$$

$$\left. \left. + 3\alpha_3^2 + 176\rho_1^2 + 80\rho_2^2 + 128\rho_1\rho_2 \right) g_R^2 + 33g_R^6 \right) \right], \tag{A.9}$$

$$\beta(\rho_2) = \frac{1}{16\pi^2} \left[3g_R^2 \left(g_R^2 - 4g_{BL}^2 \right) - \alpha_3^2 + 12\rho_2(2\rho_1 + \rho_2) - 12\rho_2 \left(2g_R^2 + g_{BL}^2 \right) \right]$$

$$+ \frac{1}{(16\pi^2)^2} \left[\frac{2}{3} \left(2g_{BL}^4 \left(143g_R^2 + 50\rho_2 \right) + 4g_{BL}^2 \left(9 \left(-4\rho_1 + 7\rho_2 \right) g_R^2 + 73g_R^4 \right. \right. \right.$$

$$+ 18 \left(2\rho_1 - \rho_2 \right) \rho_2 \right) - 3 \left(-4\alpha_3^2\rho_1 - \alpha_3^2\rho_2 + 20\alpha_1\alpha_3\rho_2 + 20\alpha_1^2\rho_2 \right.$$

$$+ 80\alpha_2^2\rho_2 - 2\alpha_3^3 - 4\alpha_1\alpha_3^2 + 3\alpha_3^2 g_L^2 - 3\alpha_3^2 h_t^2 + 8\rho_2^3 + 224\rho_1\rho_2^2 + 224\rho_1^2\rho_2 \right)$$

$$\left. \left. + 4 \left(9\rho_1 + 8\rho_2 \right) g_R^4 + 144\rho_2 \left(2\rho_1 + \rho_2 \right) g_R^2 - 119g_R^6 \right) \right], \tag{A.10}$$

$$\beta(\alpha_1) = \frac{1}{16\pi^2}\left[6g_R^4 + 4\alpha_1^2 + 16\alpha_2^2 + \alpha_3^2 + 4\alpha_1(5\lambda_1 + 2\lambda_3) + 48\alpha_2\lambda_4 + 8\alpha_3(\lambda_1 + \lambda_3)\right.$$

$$\left. + 8\alpha_1(2\rho_1 + \rho_2) + 2\alpha_3(3\rho_1 + 4\rho_2) - \frac{3}{2}\alpha_1(3g_L^2 + 11g_R^2 + 4g_{BL}^2) + 6\alpha_1 h_t^2\right]$$

$$+ \frac{1}{(16\pi^2)^2}\left[\frac{245g_R^6}{6} - 30g_R^4 g_{BL}^2 - 2g_R^2 g_{BL}^2\left(6h_t^2 - 10\alpha_1 + 19\alpha_3\right)\right.$$

$$- \frac{3}{16}g_L^4\left(\alpha_1 - 40\alpha_3\right) + g_{BL}^4\left(-4h_t^2 + \frac{268\alpha_1}{3} + 30\alpha_3\right)$$

$$+ g_R^4\left(-6h_t^2 + \frac{3647}{48}\alpha_1 + 50\alpha_3 + 100\lambda_1 + 40\lambda_3 + 80\rho_1 + 40\rho_2\right)$$

$$- \frac{3}{8}g_L^2\left(60g_R^4 - (15\alpha_1 + 4\alpha_3)g_R^2 - 2\left(15\alpha_1 h_t^2 + 4\alpha_1^2 + 16\alpha_2^2 + \alpha_3^2\right.\right.$$

$$\left.+ 64\alpha_3\lambda_1 + 64\alpha_3\lambda_3 + 32\alpha_1\left(5\lambda_1 + 2\lambda_3\right) + 384\alpha_2\lambda_4\right))$$

$$+ g_R^2\left(11\alpha_1^2 + 44\alpha_2^2 + \frac{11}{4}\alpha_3^2 + \frac{45}{4}h_t^2\alpha_1 + 120\alpha_1\lambda_1 + 60\alpha_3\lambda_1\right.$$

$$\left.+ 48\alpha_1\lambda_3 + 24\alpha_3\lambda_3 + 288\alpha_2\lambda_4 + 256\alpha_1\rho_1 + 108\alpha_3\rho_1 + 128\alpha_1\rho_2 + 104\alpha_3\rho_2\right)$$

$$+ g_{BL}^2\left(4\alpha_1^2 + 16\alpha_2^2 + \alpha_3^2 + 48\alpha_3\rho_1 + 64\alpha_3\rho_2\right.$$

$$\left.+ \alpha_1\left(\frac{5h_t^2}{6} + 32\left(4\rho_1 + 2\rho_2\right)\right)\right) - 64\alpha_1\alpha_3\rho_2 - 80\alpha_1\rho_1\rho_2 - 64\alpha_3\rho_1\rho_2$$

$$- 15\alpha_1^3 - 6\alpha_3^3 - 12h_t^2\alpha_1^2 - 48h_t^2\alpha_2^2 - 172\alpha_1\alpha_2^2 - 3h_t^2\alpha_3^2 - \frac{45}{4}\alpha_1\alpha_3^2$$

$$- 100\alpha_1\lambda_1^2 - 32\alpha_3\lambda_1^2 - 960\alpha_1\lambda_2^2 - 768\alpha_3\lambda_2^2 - 160\alpha_1\lambda_3^2 - 128\alpha_3\lambda_3^2$$

$$- 240\alpha_1\lambda_4^2 - 144\alpha_3\lambda_4^2 - 80\alpha_1\rho_1^2 - 24\alpha_3\rho_1^2 - 120\alpha_1\rho_2^2 - 96\alpha_3\rho_2^2$$

$$- 18h_t^4\alpha_1 + 40g_S^2 h_t^2\alpha_1 - 7\alpha_1^2\alpha_3 - 80\alpha_2^2\alpha_3 - 120\alpha_1^2\lambda_1 - 224\alpha_2^2\lambda_1$$

$$- 30\alpha_3^2\lambda_1 - 120h_t^2\alpha_1\lambda_1 - 48h_t^2\alpha_3\lambda_1 - 64\alpha_1\alpha_3\lambda_1 - 768\alpha_2^2\lambda_2 - 48\alpha_1^2\lambda_3$$

$$- 320\alpha_2^2\lambda_3 - 12\alpha_3^2\lambda_3 - 48h_t^2\alpha_1\lambda_3 - 48h_t^2\alpha_3\lambda_3 - 64\alpha_1\alpha_3\lambda_3 - 80\alpha_1\lambda_1\lambda_3$$

$$- 64\alpha_3\lambda_1\lambda_3 - 288h_t^2\alpha_2\lambda_4 - 576\alpha_1\alpha_2\lambda_4 - 192\alpha_2\alpha_3\lambda_4 - 576\alpha_2\lambda_1\lambda_4$$

$$- 1152\alpha_2\lambda_2\lambda_4 - 576\alpha_2\lambda_3\lambda_4 - 96\alpha_1^2\rho_1 - 384\alpha_2^2\rho_1 - 24\alpha_3^2\rho_1 - 48\alpha_1\alpha_3\rho_1$$

$$\left.- 48\alpha_1^2\rho_2 - 192\alpha_2^2\rho_2 - 12\alpha_3^2\rho_2\right], \tag{A.11}$$

$$\beta(\alpha_2) = \frac{1}{16\pi^2}\left[-\frac{3}{2}\alpha_2(3g_L^2 + 11g_R^2 + 4g_{BL}^2) + 6(2\alpha_1 + \alpha_3)\lambda_4 + 4\alpha_2(\lambda_1 + 12\lambda_2 + 4\lambda_3)\right.$$

$$\left.+ 8\alpha_2(2\rho_1 + \rho_2) + 4\alpha_2(2\alpha_1 + \alpha_3) + 6\alpha_2 h_t^2\right]$$

$$+ \frac{1}{(16\pi^2)^2}\left[-\frac{243}{16}\alpha_2 g_L^4 + \frac{45}{8}\alpha_2 g_L^2 g_R^2 + g_R^4\left(\frac{2927}{48}\alpha_2 + 60\lambda_4\right) + \frac{268}{3}\alpha_2 g_{BL}^4\right.$$

$$+ 40\alpha_2 g_S^2 h_t^2 + \frac{3}{8}g_L^2\left(2\left(4\left(\alpha_2\left(\alpha_3 + 8\lambda_1 + 96\lambda_2 + 32\lambda_3\right)\right.\right.\right.$$

$$\left.+ 12\alpha_3\lambda_4 + 2\alpha_1\left(\alpha_2 + 12\lambda_4\right)\right) + 15\alpha_2 h_t^2))$$

$$
+g_R^2 \Big(24\alpha_2\lambda_1 + 288\alpha_2\lambda_2 + 96\alpha_2\lambda_3 g_R^2 + 72\alpha_1\lambda_4 + 36\alpha_3\lambda_4 + 256\alpha_2\rho_1
$$

$$
+128\alpha_2\rho_2 + 22\alpha_1\alpha_2 + 11\alpha_2\alpha_3 + \frac{45}{4}\alpha_2 h_t^2 \Big)
$$

$$
+\frac{1}{6}\alpha_2 g_{BL}^2 \left(24\left(2\alpha_1 + \alpha_3 + 32\rho_1 + 16\rho_2\right) + 120 g_R^2 + 5h_t^2 \right)
$$

$$
-36\alpha_2\lambda_1^2 + 192\alpha_2\lambda_2^2 - 240\alpha_2\lambda_4^2 - 112\alpha_1\alpha_2\lambda_1 - 56\alpha_2\alpha_3\lambda_1 - 384\alpha_1\alpha_2\lambda_2
$$

$$
-192\alpha_2\alpha_3\lambda_2 - 384\alpha_2\lambda_1\lambda_2 - 160\alpha_1\alpha_2\lambda_3 - 80\alpha_2\alpha_3\lambda_3 - 144\alpha_2\lambda_1\lambda_3
$$

$$
-384\alpha_2\lambda_2\lambda_3 - 72\alpha_1^2\lambda_4 - 288\alpha_2^2\lambda_4 - 30\alpha_3^2\lambda_4 - 72\alpha_1\alpha_3\lambda_4 - 144\alpha_1\lambda_1\lambda_4
$$

$$
-72\alpha_3\lambda_1\lambda_4 - 288\alpha_1\lambda_2\lambda_4 - 144\alpha_3\lambda_2\lambda_4 - 144\alpha_1\lambda_3\lambda_4
$$

$$
-72\alpha_3\lambda_3\lambda_4 - 80\alpha_2\rho_1^2 - 120\alpha_2\rho_2^2 - 192\alpha_1\alpha_2\rho_1 - 96\alpha_2\alpha_3\rho_1 - 96\alpha_1\alpha_2\rho_2
$$

$$
-48\alpha_2\alpha_3\rho_2 - 80\alpha_2\rho_1\rho_2 - 60\alpha_2^3 - \frac{49}{4}\alpha_2\alpha_3^2 - 43\alpha_1^2\alpha_2 - 43\alpha_1\alpha_2\alpha_3 - 30\alpha_2 h_t^4
$$

$$
-12h_t^2\left(2\alpha_2\lambda_1 + 24\alpha_2\lambda_2 + 8\alpha_2\lambda_3 + 6\alpha_1\lambda_4 + 3\alpha_3\lambda_4 + 2\alpha_1\alpha_2 + \alpha_2\alpha_3\right) \bigg], \quad \text{(A.12)}
$$

$$
\beta(\alpha_3) = \frac{1}{16\pi^2}\bigg[4\alpha_3^2 - \frac{3}{2}\alpha_3\left(3g_L^2 + 11g_R^2 + 4g_{BL}^2\right) + 8\alpha_1\alpha_3 + 4\alpha_3(\lambda_1 - 2\lambda_3)
$$

$$
+4\alpha_3(\rho_1 - 2\rho_2) + 6\alpha_3 h_t^2 \bigg]
$$

$$
+\frac{1}{(16\pi^2)^2}\bigg[\frac{88}{3}\alpha_3 g_{BL}^4 + \frac{1}{6}g_{BL}^2\left(144 g_R^2\left(4\alpha_3 + h_t^2\right)\right.
$$

$$
+\alpha_3\left(24\left(2\alpha_1 + \alpha_3 + 8\left(\rho_1 - 2\rho_2\right)\right) + 5h_t^2\right)\big)
$$

$$
-\frac{1}{48}\alpha_3\left(-18g_L^2\left(16\alpha_1 + 8\alpha_3 + 7g_R^2 + 30h_t^2 + 64\lambda_1 - 128\lambda_3\right)\right.
$$

$$
-12g_R^2\left(88\alpha_1 + 44\alpha_3 + 45h_t^2 + 160\rho_1 - 320\rho_2\right)
$$

$$
-12\left(-448\alpha_1\lambda_1 - 224\alpha_3\lambda_1 + 128\alpha_1\lambda_3 + 64\alpha_3\lambda_3 - 768\alpha_2\lambda_4\right.
$$

$$
-384\alpha_1\rho_1 - 192\alpha_3\rho_1 + 128\alpha_1\rho_2 + 64\alpha_3\rho_2 - 124\alpha_1^2
$$

$$
-48\alpha_2^2 - 29\alpha_3^2 - 124\alpha_1\alpha_3 + 160g_S^2 h_t^2 + 384\lambda_3^2 + 192\lambda_4^2
$$

$$
-48\left(2\alpha_1 + \alpha_3 + 2\lambda_1 - 4\lambda_3\right)h_t^2 - 72h_t^4 - 144\lambda_1^2 + 2304\lambda_2^2
$$

$$
+192\lambda_1\lambda_3 - 128\rho_1^2 + 288\rho_2^2 + 192\rho_1\rho_2\big) + 729g_L^4 + 1153g_R^4\big) \bigg], \quad \text{(A.13)}
$$

$$
\beta(h_t) = \frac{1}{16\pi^2}\bigg[-h_t\left(8g_S^2 + \frac{9}{4}g_L^2 + \frac{9}{4}g_R^2 + \frac{1}{6}g_{BL}^2\right) + 5h_t^3 \bigg]
$$

$$
+\frac{1}{(16\pi^2)^2}\bigg[-\frac{1}{144}h_t\bigg(-g_{BL}^2\left(4\left(-8g_S^2 + 31h_t^2\right) + 27g_L^2 + 27g_R^2\right)
$$

$$
-97g_{BL}^4 + 3\left(9g_L^2\left(27g_R^2 - 48g_S^2 - 86h_t^2\right)\right.
$$

$$
+2\left(-9g_R^2\left(24g_S^2 + 43h_t^2\right) - 992g_S^2 h_t^2 + 78g_R^4 + 2592g_S^4\right.
$$

$$
+3\left(-12\alpha_1^2 - 48\alpha_2^2 - 9\alpha_3^2 - 12\alpha_1\alpha_3 + 64\left(2\lambda_1 - \lambda_3\right)h_t^2\right.
$$

$$
+136h_t^4 - 80\lambda_1^2 - 768\lambda_2^2 - 128\lambda_3^2 - 192\lambda_4^2 - 64\lambda_1\lambda_3\big)\big) + 252g_L^4\big)\bigg)\bigg]. \quad \text{(A.14)}
$$

To see how the fermions get their masses in the LRSM, we write down the Yukawa Lagrangian:

$$\mathcal{L}_Y = h^q \bar{Q}_L \Phi Q_R + \tilde{h}^q \bar{Q}_L \tilde{\Phi} Q_R + h^\ell \bar{\psi}_L \Phi \psi_R + \tilde{h}^\ell \bar{\psi}_L \tilde{\Phi} \psi_R$$
$$+ f_R \psi_R^\mathsf{T} C i \tau_2 \Delta_R \psi_R \; + \; \text{H.c.} \tag{A.15}$$

where $\tilde{\Phi} = \sigma_2 \Phi^* \sigma_2$ (σ_2 being the second Pauli matrix) and $C = i\gamma_2 \gamma_0$ is the charge conjugation operator (γ_μ being the Dirac matrices). After symmetry breaking, the quark and charged lepton masses are given by the generic formulas $M_u = h^q \kappa + \tilde{h}^q \kappa'$ for up-type quarks, $M_d = h^q \kappa' + \tilde{h}^q \kappa$ for down-type quarks, and similarly for the charged leptons, where we have neglected CP violation in the fermion matrices. To account for the SM fermion hierarchy, we set $\kappa'/\kappa \simeq m_b/m_t \simeq 1/60$, then the top and bottom quark masses are respectively

$$m_t \simeq h_{33}^q \kappa \simeq h_{33}^q v_{\text{EW}} \,, \quad m_b \simeq h_{33}^q \kappa' + \tilde{h}_{33}^q \kappa \,, \tag{A.16}$$

with h_{33}^q and $\tilde{h}_{33}^q$ the (3, 3) elements of the h^q and $\tilde{h}^q$ matrices. It is expected that for the bottom quark mass $\tilde{h}_{33}^q \ll h_{33}^q \sim \mathcal{O}(1)$. With the first two generation quarks much lighter than the third generation in the SM, we consider only the RG running of $h_t = h_{33}^q$ in the quark sector, as shown in eq. (A.14).

In the lepton sector, the tauon mass $m_\tau \simeq h_{33}^\ell \kappa' + \tilde{h}_{33}^\ell \kappa$ (h_{33}^ℓ and $\tilde{h}_{33}^\ell$ are respectively the (3, 3) elements of the h^ℓ and $\tilde{h}^\ell$ matrices), which is closely related to the Dirac mass matrix for neutrinos $m_D = h^\ell \kappa + \tilde{h}^\ell \kappa'$. The elements h_{33}^ℓ and $\tilde{h}_{33}^\ell$ cannot be very large for TeV-scale RHNs, or we need fine-tuning or large cancellation in fitting the charged lepton masses and the tiny neutrino masses. Thus we have neglected also the matrices h^ℓ and $\tilde{h}^\ell$ in the β-functions above. For the RH scale $v_R \gtrsim 10\,\text{TeV}$, as implied by the scalar perturbativity constraints in figures 7 and 8, if the RHNs are all the TeV-scale, say $M_N \simeq 1\,\text{TeV}$, the Yukawa coupling $f_R \sim M_N/v_R \lesssim 0.1$, and we do not include it either in the β-functions above.

References

[1] H. Georgi, *The State of the Art in Gauge Theories*, *AIP Conf. Proc.* **23** (1975) 575.

[2] H. Fritzsch and P. Minkowski, *Unified Interactions of Leptons and Hadrons*, *Annals Phys.* **93** (1975) 193 [ɪɴSPIRE].

[3] M.S. Chanowitz, J.R. Ellis and M.K. Gaillard, *The Price of Natural Flavor Conservation in Neutral Weak Interactions*, *Nucl. Phys.* **B 128** (1977) 506 [ɪɴSPIRE].

[4] H. Georgi and D.V. Nanopoulos, *Ordinary Predictions from Grand Principles: T Quark Mass in* O(10), *Nucl. Phys.* **B 155** (1979) 52 [ɪɴSPIRE].

[5] K.S. Babu and R.N. Mohapatra, *Predictive neutrino spectrum in minimal* SO(10) *grand unification*, *Phys. Rev. Lett.* **70** (1993) 2845 [hep-ph/9209215] [ɪɴSPIRE].

[6] R.E. Marshak and R.N. Mohapatra, *Quark-Lepton Symmetry and B-L as the* U(1) *Generator of the Electroweak Symmetry Group*, *Phys. Lett.* **B 91** (1980) 222 [INSPIRE].

[7] R.N. Mohapatra and R.E. Marshak, *Local B-L Symmetry of Electroweak Interactions, Majorana Neutrinos and Neutron Oscillations*, *Phys. Rev. Lett.* **44** (1980) 1316 [*Erratum ibid.* **44** (1980) 1643] [INSPIRE].

[8] N.G. Deshpande and D. Iskandar, *Study of the Gauge Group* SU(2)$_L$ × T(3)$_R$ × U(1) − V, *Nucl. Phys.* **B 167** (1980) 223 [INSPIRE].

[9] P. Galison and A. Manohar, *Two Z's or not two Z's?*, *Phys. Lett.* **B 136** (1984) 279 [INSPIRE].

[10] J.C. Pati and A. Salam, *Lepton Number as the Fourth Color*, *Phys. Rev.* **D 10** (1974) 275 [*Erratum ibid.* **D 11** (1975) 703] [INSPIRE].

[11] R.N. Mohapatra and J.C. Pati, *A Natural Left-Right Symmetry*, *Phys. Rev.* **D 11** (1975) 2558 [INSPIRE].

[12] G. Senjanović and R.N. Mohapatra, *Exact Left-Right Symmetry and Spontaneous Violation of Parity*, *Phys. Rev.* **D 12** (1975) 1502 [INSPIRE].

[13] P. Minkowski, $\mu \to e\gamma$ *at a Rate of One Out of* 10^9 *Muon Decays?*, *Phys. Lett.* **B 67** (1977) 421 [INSPIRE].

[14] R.N. Mohapatra and G. Senjanović, *Neutrino Mass and Spontaneous Parity Nonconservation*, *Phys. Rev. Lett.* **44** (1980) 912 [INSPIRE].

[15] T. Yanagida, *Horizontal gauge symmetry and masses of neutrinos*, *Conf. Proc.* **C 7902131** (1979) 95 [INSPIRE].

[16] M. Gell-Mann, P. Ramond and R. Slansky, *Complex Spinors and Unified Theories*, *Conf. Proc.* **C 790927** (1979) 315 [arXiv:1306.4669] [INSPIRE].

[17] S.L. Glashow, *The Future of Elementary Particle Physics*, *NATO Sci. Ser.* **B 61** (1980) 687.

[18] L.B. Okun, *Limits of electrodynamics: paraphotons?*, *Sov. Phys. JETP* **56** (1982) 502 [INSPIRE].

[19] B. Holdom, *Two* U(1)′*s and Epsilon Charge Shifts*, *Phys. Lett.* **B 166** (1986) 196 [INSPIRE].

[20] R. Foot and X.-G. He, *Comment on Z Z-prime mixing in extended gauge theories*, *Phys. Lett.* **B 267** (1991) 509 [INSPIRE].

[21] W. Buchmüller, C. Greub and P. Minkowski, *Neutrino masses, neutral vector bosons and the scale of B-L breaking*, *Phys. Lett.* **B 267** (1991) 395 [INSPIRE].

[22] L. Basso, *Phenomenology of the minimal B-L extension of the Standard Model at the LHC*, Ph.D. Thesis, Southampton University, Southampton U.K. (2011) [arXiv:1106.4462] [INSPIRE].

[23] T. Appelquist, B.A. Dobrescu and A.R. Hopper, *Nonexotic neutral gauge bosons*, *Phys. Rev.* **D 68** (2003) 035012 [hep-ph/0212073] [INSPIRE].

[24] M. Carena, A. Daleo, B.A. Dobrescu and T.M.P. Tait, Z' *gauge bosons at the Tevatron*, *Phys. Rev.* **D 70** (2004) 093009 [hep-ph/0408098] [INSPIRE].

[25] A. Das, S. Oda, N. Okada and D.-s. Takahashi, *Classically conformal* U(1)′ *extended standard model, electroweak vacuum stability and LHC Run-2 bounds*, *Phys. Rev.* **D 93** (2016) 115038 [arXiv:1605.01157] [INSPIRE].

[26] S. Oda, N. Okada and D.-s. Takahashi, *Right-handed neutrino dark matter in the classically conformal* U(1)′ *extended standard model*, *Phys. Rev.* **D 96** (2017) 095032 [arXiv:1704.05023] [INSPIRE].

[27] J. Alexander et al., *Dark Sectors 2016 Workshop: Community Report*, 2016, arXiv:1608.08632, http://lss.fnal.gov/archive/2016/conf/fermilab-conf-16-421.pdf [INSPIRE].

[28] P. Langacker, *The Physics of Heavy* Z′ *Gauge Bosons*, *Rev. Mod. Phys.* **81** (2009) 1199 [arXiv:0801.1345] [INSPIRE].

[29] CMS collaboration, *Search for a heavy right-handed W boson and a heavy neutrino in events with two same-flavor leptons and two jets at* $\sqrt{s} = 13\,TeV$, *JHEP* **05** (2018) 148 [arXiv:1803.11116] [INSPIRE].

[30] ATLAS collaboration, *Search for heavy Majorana or Dirac neutrinos and right-handed W gauge bosons in final states with two charged leptons and two jets at* $\sqrt{s} = 13\,TeV$ *with the ATLAS detector*, *JHEP* **01** (2019) 016 [arXiv:1809.11105] [INSPIRE].

[31] ATLAS collaboration, *Search for new high-mass resonances in the dilepton final state using proton-proton collisions at* $\sqrt{s} = 13\,TeV$ *with the ATLAS detector*, ATLAS-CONF-2016-045 (2016).

[32] CMS collaboration, *Search for a high-mass resonance decaying into a dilepton final state in* $13\,fb^{-1}$ *of pp collisions at* $\sqrt{s} = 13\,TeV$, CMS-PAS-EXO-16-031 (2016).

[33] A. Ferrari et al., *Sensitivity study for new gauge bosons and right-handed Majorana neutrinos in pp collisions at* $s = 14\text{-}TeV$, *Phys. Rev.* **D 62** (2000) 013001 [INSPIRE].

[34] T.G. Rizzo, *Exploring new gauge bosons at a* $100\,TeV$ *collider*, *Phys. Rev.* **D 89** (2014) 095022 [arXiv:1403.5465] [INSPIRE].

[35] P.S.B. Dev, D. Kim and R.N. Mohapatra, *Disambiguating Seesaw Models using Invariant Mass Variables at Hadron Colliders*, *JHEP* **01** (2016) 118 [arXiv:1510.04328] [INSPIRE].

[36] M. Mitra, R. Ruiz, D.J. Scott and M. Spannowsky, *Neutrino Jets from High-Mass* W_R *Gauge Bosons in TeV-Scale Left-Right Symmetric Models*, *Phys. Rev.* **D 94** (2016) 095016 [arXiv:1607.03504] [INSPIRE].

[37] R. Ruiz, *Lepton Number Violation at Colliders from Kinematically Inaccessible Gauge Bosons*, *Eur. Phys. J.* **C 77** (2017) 375 [arXiv:1703.04669] [INSPIRE].

[38] N. Arkani-Hamed, T. Han, M. Mangano and L.-T. Wang, *Physics opportunities of a* $100\,TeV$ *proton-proton collider*, *Phys. Rept.* **652** (2016) 1 [arXiv:1511.06495] [INSPIRE].

[39] T. Golling et al., *Physics at a* $100\,TeV$ *pp collider: beyond the Standard Model phenomena*, *CERN Yellow Report* (2017) 441 [arXiv:1606.00947] [INSPIRE].

[40] PARTICLE DATA GROUP collaboration, *Review of Particle Physics*, *Phys. Rev.* **D 98** (2018) 030001 [INSPIRE].

[41] G. Ecker, W. Grimus and H. Neufeld, *Higgs Induced Flavor Changing Neutral Interactions in* $SU(2)_L \times SU(2)_R \times U(1)$, *Phys. Lett.* **B 127** (1983) 365 [*Erratum ibid.* **B 132** (1983) 467] [INSPIRE].

[42] Y. Zhang, H. An, X. Ji and R.N. Mohapatra, *General CP-violation in Minimal Left-Right Symmetric Model and Constraints on the Right-Handed Scale*, *Nucl. Phys.* **B 802** (2008) 247 [arXiv:0712.4218] [INSPIRE].

[43] A. Maiezza, M. Nemevšek, F. Nesti and G. Senjanović, *Left-Right Symmetry at LHC*, *Phys. Rev.* **D 82** (2010) 055022 [arXiv:1005.5160] [INSPIRE].

[44] S. Bertolini, A. Maiezza and F. Nesti, *Present and Future K and B Meson Mixing Constraints on TeV Scale Left-Right Symmetry*, *Phys. Rev.* **D 89** (2014) 095028 [arXiv:1403.7112] [INSPIRE].

[45] M. Singer, J.W.F. Valle and J. Schechter, *Canonical Neutral Current Predictions From the Weak Electromagnetic Gauge Group* SU(3) × U(1), *Phys. Rev.* **D 22** (1980) 738 [INSPIRE].

[46] P.H. Frampton, *Chiral dilepton model and the flavor question*, *Phys. Rev. Lett.* **69** (1992) 2889 [INSPIRE].

[47] F. Pisano and V. Pleitez, *An* SU(3) × U(1) *model for electroweak interactions*, *Phys. Rev.* **D 46** (1992) 410 [hep-ph/9206242] [INSPIRE].

[48] R. Foot, O.F. Hernandez, F. Pisano and V. Pleitez, *Lepton masses in an* SU(3) − L × U(1) − N *gauge model*, *Phys. Rev.* **D 47** (1993) 4158 [hep-ph/9207264] [INSPIRE].

[49] A.G. Dias, C.A. de S. Pires and P.S. Rodrigues da Silva, *The Left-Right* SU(3)$_L$ × SU(3)$_R$ × U(1)$_X$ *Model with Light, keV and Heavy Neutrinos*, *Phys. Rev.* **D 82** (2010) 035013 [arXiv:1003.3260] [INSPIRE].

[50] M. Reig, J.W.F. Valle and C.A. Vaquera-Araujo, *Unifying left-right symmetry and 331 electroweak theories*, *Phys. Lett.* **B 766** (2017) 35 [arXiv:1611.02066] [INSPIRE].

[51] M. Reig, J.W.F. Valle and C.A. Vaquera-Araujo, *Three-family left-right symmetry with low-scale seesaw mechanism*, *JHEP* **05** (2017) 100 [arXiv:1611.04571] [INSPIRE].

[52] D. Borah and S. Patra, *Universal seesaw and* 0νββ *in new 3331 left-right symmetric model*, *Phys. Lett.* **B 771** (2017) 318 [arXiv:1701.08675] [INSPIRE].

[53] C. Hati, S. Patra, M. Reig, J.W.F. Valle and C.A. Vaquera-Araujo, *Towards gauge coupling unification in left-right symmetric* SU(3)$_c$ × SU(3)$_L$ × SU(3)$_R$ × U(1)$_X$ *theories*, *Phys. Rev.* **D 96** (2017) 015004 [arXiv:1703.09647] [INSPIRE].

[54] Z.G. Berezhiani, *The Weak Mixing Angles in Gauge Models with Horizontal Symmetry: A New Approach to Quark and Lepton Masses*, *Phys. Lett.* **B 129** (1983) 99 [INSPIRE].

[55] D. Chang and R.N. Mohapatra, *Small and Calculable Dirac Neutrino Mass*, *Phys. Rev. Lett.* **58** (1987) 1600 [INSPIRE].

[56] S. Rajpoot, *See-saw masses for quarks and leptons in an ambidextrous electroweak interaction model*, *Mod. Phys. Lett.* **A 2** (1987) 307 [*Erratum ibid.* **A 2** (1987) 541] [INSPIRE].

[57] A. Davidson and K.C. Wali, *Universal Seesaw Mechanism?*, *Phys. Rev. Lett.* **59** (1987) 393 [INSPIRE].

[58] K.S. Babu and R.N. Mohapatra, *CP Violation in Seesaw Models of Quark Masses*, *Phys. Rev. Lett.* **62** (1989) 1079 [INSPIRE].

[59] K.S. Babu and R.N. Mohapatra, *A Solution to the Strong CP Problem Without an Axion*, *Phys. Rev.* **D 41** (1990) 1286 [INSPIRE].

[60] R.N. Mohapatra and Y. Zhang, *TeV Scale Universal Seesaw, Vacuum Stability and Heavy Higgs*, *JHEP* **06** (2014) 072 [`arXiv:1401.6701`] [INSPIRE].

[61] P.S.B. Dev, R.N. Mohapatra and Y. Zhang, *Quark Seesaw, Vectorlike Fermions and Diphoton Excess*, *JHEP* **02** (2016) 186 [`arXiv:1512.08507`] [INSPIRE].

[62] F.F. Deppisch, C. Hati, S. Patra, P. Pritimita and U. Sarkar, *Neutrinoless double beta decay in left-right symmetric models with a universal seesaw mechanism*, *Phys. Rev.* **D 97** (2018) 035005 [`arXiv:1701.02107`] [INSPIRE].

[63] A. Patra and S.K. Rai, *Lepton-specific universal seesaw model with left-right symmetry*, *Phys. Rev.* **D 98** (2018) 015033 [`arXiv:1711.00627`] [INSPIRE].

[64] P.S. Bhupal Dev, R.N. Mohapatra and Y. Zhang, *Naturally stable right-handed neutrino dark matter*, *JHEP* **11** (2016) 077 [`arXiv:1608.06266`] [INSPIRE].

[65] P.S.B. Dev, R.N. Mohapatra and Y. Zhang, *Heavy right-handed neutrino dark matter in left-right models*, *Mod. Phys. Lett.* **A 32** (2017) 1740007 [`arXiv:1610.05738`] [INSPIRE].

[66] J.L. Hewett and T.G. Rizzo, *Low-Energy Phenomenology of Superstring Inspired E_6 Models*, *Phys. Rept.* **183** (1989) 193 [INSPIRE].

[67] H. Georgi and S. Weinberg, *Neutral Currents in Expanded Gauge Theories*, *Phys. Rev.* **D 17** (1978) 275 [INSPIRE].

[68] P.S.B. Dev, R.N. Mohapatra and Y. Zhang, *Probing the Higgs Sector of the Minimal Left-Right Symmetric Model at Future Hadron Colliders*, *JHEP* **05** (2016) 174 [`arXiv:1602.05947`] [INSPIRE].

[69] J. Brehmer, J. Hewett, J. Kopp, T. Rizzo and J. Tattersall, *Symmetry Restored in Dibosons at the LHC?*, *JHEP* **10** (2015) 182 [`arXiv:1507.00013`] [INSPIRE].

[70] P.S.B. Dev, R.N. Mohapatra and Y. Zhang, *Long Lived Light Scalars as Probe of Low Scale Seesaw Models*, *Nucl. Phys.* **B 923** (2017) 179 [`arXiv:1703.02471`] [INSPIRE].

[71] P.S.B. Dev, R.N. Mohapatra and Y. Zhang, *Leptogenesis constraints on $B - L$ breaking Higgs boson in TeV scale seesaw models*, *JHEP* **03** (2018) 122 [`arXiv:1711.07634`] [INSPIRE].

[72] S. Patra, F.S. Queiroz and W. Rodejohann, *Stringent Dilepton Bounds on Left-Right Models using LHC data*, *Phys. Lett.* **B 752** (2016) 186 [`arXiv:1506.03456`] [INSPIRE].

[73] M. Lindner, F.S. Queiroz and W. Rodejohann, *Dilepton bounds on left-right symmetry at the LHC run II and neutrinoless double beta decay*, *Phys. Lett.* **B 762** (2016) 190 [`arXiv:1604.07419`] [INSPIRE].

[74] R. Diener, S. Godfrey and T.A.W. Martin, *Unravelling an Extra Neutral Gauge Boson at the LHC using Third Generation Fermions*, *Phys. Rev.* **D 83** (2011) 115008 [`arXiv:1006.2845`] [INSPIRE].

[75] S. Godfrey and T. Martin, *Z' Discovery Reach at Future Hadron Colliders: A Snowmass White Paper*, in *Proceedings of 2013 Community Summer Study on the Future of U.S. Particle Physics: Snowmass on the Mississippi (CSS2013)*, Minneapolis U.S.A. (2013) [`arXiv:1309.1688`] [INSPIRE].

[76] W. Konetschny and W. Kummer, *Nonconservation of Total Lepton Number with Scalar Bosons*, *Phys. Lett.* **B 70** (1977) 433 [INSPIRE].

[77] M. Magg and C. Wetterich, *Neutrino Mass Problem and Gauge Hierarchy*, *Phys. Lett.* **B 94** (1980) 61 [INSPIRE].

[78] J. Schechter and J.W.F. Valle, *Neutrino Masses in* SU(2) × U(1) *Theories*, *Phys. Rev.* **D 22** (1980) 2227 [INSPIRE].

[79] T.P. Cheng and L.-F. Li, *Neutrino Masses, Mixings and Oscillations in* SU(2) × U(1) *Models of Electroweak Interactions*, *Phys. Rev.* **D 22** (1980) 2860 [INSPIRE].

[80] R.N. Mohapatra and G. Senjanović, *Neutrino Masses and Mixings in Gauge Models with Spontaneous Parity Violation*, *Phys. Rev.* **D 23** (1981) 165 [INSPIRE].

[81] G. Lazarides, Q. Shafi and C. Wetterich, *Proton Lifetime and Fermion Masses in an* SO(10) *Model*, *Nucl. Phys.* **B 181** (1981) 287 [INSPIRE].

[82] F.F. Deppisch, T.E. Gonzalo, S. Patra, N. Sahu and U. Sarkar, *Double beta decay, lepton flavor violation and collider signatures of left-right symmetric models with spontaneous D-parity breaking*, *Phys. Rev.* **D 91** (2015) 015018 [arXiv:1410.6427] [INSPIRE].

[83] P.S. Bhupal Dev and R.N. Mohapatra, *Unified explanation of the* eejj, *diboson and dijet resonances at the LHC*, *Phys. Rev. Lett.* **115** (2015) 181803 [arXiv:1508.02277] [INSPIRE].

[84] D. Chang, R.N. Mohapatra and M.K. Parida, *Decoupling Parity and* SU(2)$_R$ *Breaking Scales: A New Approach to Left-Right Symmetric Models*, *Phys. Rev. Lett.* **52** (1984) 1072 [INSPIRE].

[85] F. Lyonnet, I. Schienbein, F. Staub and A. Wingerter, *PyR@TE: Renormalization Group Equations for General Gauge Theories*, *Comput. Phys. Commun.* **185** (2014) 1130 [arXiv:1309.7030] [INSPIRE].

[86] F. Lyonnet, *Automation of non-SUSY two-loop RGEs with PyR@TE: latest developments*, in *Proceedings, Meeting of the APS Division of Particles and Fields (DPF 2015)*, Ann Arbor U.S.A. (2015) [arXiv:1510.08841] [INSPIRE].

[87] W.-Y. Keung and G. Senjanović, *Majorana Neutrinos and the Production of the Right-handed Charged Gauge Boson*, *Phys. Rev. Lett.* **50** (1983) 1427 [INSPIRE].

[88] C.-Y. Chen, P.S.B. Dev and R.N. Mohapatra, *Probing Heavy-Light Neutrino Mixing in Left-Right Seesaw Models at the LHC*, *Phys. Rev.* **D 88** (2013) 033014 [arXiv:1306.2342] [INSPIRE].

[89] F.F. Deppisch, P.S. Bhupal Dev and A. Pilaftsis, *Neutrinos and Collider Physics*, *New J. Phys.* **17** (2015) 075019 [arXiv:1502.06541] [INSPIRE].

[90] G. Senjanović and V. Tello, *Right Handed Quark Mixing in Left-Right Symmetric Theory*, *Phys. Rev. Lett.* **114** (2015) 071801 [arXiv:1408.3835] [INSPIRE].

[91] G. Beall, M. Bander and A. Soni, *Constraint on the Mass Scale of a Left-Right Symmetric Electroweak Theory from the K(L) K(S) Mass Difference*, *Phys. Rev. Lett.* **48** (1982) 848 [INSPIRE].

[92] R.N. Mohapatra, G. Senjanović and M.D. Tran, *Strangeness Changing Processes and the Limit on the Right-handed Gauge Boson Mass*, *Phys. Rev.* **D 28** (1983) 546 [INSPIRE].

[93] G. Ecker and W. Grimus, *CP Violation and Left-Right Symmetry*, *Nucl. Phys.* **B 258** (1985) 328 [INSPIRE].

[94] R.N. Mohapatra and J.D. Vergados, *A New Contribution to Neutrinoless Double Beta Decay in Gauge Models*, *Phys. Rev. Lett.* **47** (1981) 1713 [INSPIRE].

[95] M. Hirsch, H.V. Klapdor-Kleingrothaus and O. Panella, *Double beta decay in left-right symmetric models*, *Phys. Lett.* **B 374** (1996) 7 [hep-ph/9602306] [INSPIRE].

[96] V. Tello, M. Nemevšek, F. Nesti, G. Senjanović and F. Vissani, *Left-Right Symmetry: from LHC to Neutrinoless Double Beta Decay*, *Phys. Rev. Lett.* **106** (2011) 151801 [arXiv:1011.3522] [INSPIRE].

[97] J. Chakrabortty, H.Z. Devi, S. Goswami and S. Patra, *Neutrinoless double-β decay in TeV scale Left-Right symmetric models*, *JHEP* **08** (2012) 008 [arXiv:1204.2527] [INSPIRE].

[98] J. Barry and W. Rodejohann, *Lepton number and flavour violation in TeV-scale left-right symmetric theories with large left-right mixing*, *JHEP* **09** (2013) 153 [arXiv:1303.6324] [INSPIRE].

[99] P.S. Bhupal Dev, S. Goswami, M. Mitra and W. Rodejohann, *Constraining Neutrino Mass from Neutrinoless Double Beta Decay*, *Phys. Rev.* **D 88** (2013) 091301 [arXiv:1305.0056] [INSPIRE].

[100] W.-C. Huang and J. Lopez-Pavon, *On neutrinoless double beta decay in the minimal left-right symmetric model*, *Eur. Phys. J.* **C 74** (2014) 2853 [arXiv:1310.0265] [INSPIRE].

[101] P.S. Bhupal Dev, S. Goswami and M. Mitra, *TeV Scale Left-Right Symmetry and Large Mixing Effects in Neutrinoless Double Beta Decay*, *Phys. Rev.* **D 91** (2015) 113004 [arXiv:1405.1399] [INSPIRE].

[102] G. Bambhaniya, P.S.B. Dev, S. Goswami and M. Mitra, *The Scalar Triplet Contribution to Lepton Flavour Violation and Neutrinoless Double Beta Decay in Left-Right Symmetric Model*, *JHEP* **04** (2016) 046 [arXiv:1512.00440] [INSPIRE].

[103] M. Nemevšek, F. Nesti and G. Popara, *Keung-Senjanović process at the LHC: From lepton number violation to displaced vertices to invisible decays*, *Phys. Rev.* **D 97** (2018) 115018 [arXiv:1801.05813] [INSPIRE].

[104] A. Belyaev, N.D. Christensen and A. Pukhov, *CalcHEP 3.4 for collider physics within and beyond the Standard Model*, *Comput. Phys. Commun.* **184** (2013) 1729 [arXiv:1207.6082] [INSPIRE].

[105] I.Z. Rothstein, *Renormalization group analysis of the minimal left-right symmetric model*, *Nucl. Phys.* **B 358** (1991) 181 [INSPIRE].

[106] J. Chakrabortty, P. Konar and T. Mondal, *Constraining a class of B-L extended models from vacuum stability and perturbativity*, *Phys. Rev.* **D 89** (2014) 056014 [arXiv:1308.1291] [INSPIRE].

[107] J. Chakrabortty, J. Gluza, T. Jelinski and T. Srivastava, *Theoretical constraints on masses of heavy particles in Left-Right Symmetric Models*, *Phys. Lett.* **B 759** (2016) 361 [arXiv:1604.06987] [INSPIRE].

[108] A. Maiezza, G. Senjanović and J.C. Vasquez, *Higgs sector of the minimal left-right symmetric theory*, *Phys. Rev.* **D 95** (2017) 095004 [arXiv:1612.09146] [INSPIRE].

[109] P. Bhupal Dev, R.N. Mohapatra and Y. Zhang, *Displaced photon signal from a possible light scalar in minimal left-right seesaw model*, *Phys. Rev.* **D 95** (2017) 115001 [arXiv:1612.09587] [INSPIRE].

[110] ATLAS collaboration, *Search for doubly charged Higgs boson production in multi-lepton final states with the ATLAS detector using proton–proton collisions at $\sqrt{s} = 13$ TeV*, *Eur. Phys. J.* **C 78** (2018) 199 [arXiv:1710.09748] [INSPIRE].

[111] CMS collaboration, *A search for doubly-charged Higgs boson production in three and four lepton final states at $\sqrt{s} = 13$ TeV*, CMS-PAS-HIG-16-036 (2016).

[112] P.S. Bhupal Dev and Y. Zhang, *Displaced vertex signatures of doubly charged scalars in the type-II seesaw and its left-right extensions*, *JHEP* **10** (2018) 199 [arXiv:1808.00943] [INSPIRE].

[113] ATLAS and CMS collaborations, *Combined Measurement of the Higgs Boson Mass in pp Collisions at $\sqrt{s} = 7$ and $8\,TeV$ with the ATLAS and CMS Experiments*, *Phys. Rev. Lett.* **114** (2015) 191803 [arXiv:1503.07589] [INSPIRE].

[114] P.S. Bhupal Dev, R.N. Mohapatra, W. Rodejohann and X.-J. Xu, *Vacuum structure of the left-right symmetric model*, arXiv:1811.06869 [INSPIRE].

[115] J. Chakrabortty, P. Konar and T. Mondal, *Copositive Criteria and Boundedness of the Scalar Potential*, *Phys. Rev.* **D 89** (2014) 095008 [arXiv:1311.5666] [INSPIRE].